https://doi.org/10.5194/egusphere-2026-5313
Preprint. Discussion started: 9 November 2026
© Author(s) 2026. CC BY 4.0 License.

GEB-PlantFATE v1.0 Coupling of forest demographic and soil hydrological models for simulating the hydrological impacts of afforestation and biodiversity

Elisa Z. Stefaniak[1], Jaideep Joshi[2,3,4], Silvia Artuso[5], Tania L. Maxwell[1,6]., Mikhail Smilovic[5], Florian Hofhansl[1*], Jens A. de Bruijn[5,7*].

1 Biodiversity, Ecology and Conservation Group, Biodiversity and Natural Resources Program, International Institute for Applied Systems Analysis (IIASA), Laxenburg 2361, Austria

2 Advancing Systems Analysis Program, International Institute for Applied Systems Analysis, 2361 Laxenburg, Austria

3 Centre for Climate Studies, Indian Institute of Technology Bombay, Mumbai 400076, India

4 Complexity Science and Evolution Unit, Okinawa Institute of Science and Technology Graduate University, Onna, Okinawa 904-0495, Japan

5 Water Security Research Group, Biodiversity and Natural Resources Program, International Institute for Applied Systems Analysis (IIASA), Laxenburg 2361, Austria

6 Université Paris-Saclay, CNRS, AgroParisTech, Ecologie Systématique et Evolution, Gif-sur-Yvette, France

7 Institute for Environmental Studies, VU University, De Boelelaan 1087, 1081HV, Amsterdam, The Netherlands

* These authors jointly supervised this work.

Correspondence to: Elisa Z. Stefaniak (stefaniak@iiasa.ac.at)

Abstract. Forests play a significant role in the hydrological cycle by increasing water use through tree transpiration, reducing soil evaporation, providing local cooling, and altering soil hydrological properties. The nature of these interactions depends on individual tree species' functional traits, intra- and interspecific interactions, and stand age. In the short term, individuals acclimate to local conditions by adjusting their photosynthetic activity in response to temperature and water availability. As such, over time, changes in forest cover, whether through afforestation or deforestation, will affect water availability in the forest and downstream. To simultaneously predict basin-level water and carbon dynamics, representations of vegetation in hydrological models must capture processes such as soil-water-plant interactions, plant acclimation, forest dynamics, and diversity in forest age and species composition.

In this paper we advanced the capability of the Geographical Environmental and Behavioural model (GEB), a hydrological model with agent-based representations of management decisions, by coupling it with the Plant Functional Acclimation and Trait Evolution model (PlantFATE), a dynamic trait-based vegetation model built on eco-evolutionary principles, to improve hydrological response to changes in forest cover and composition. We evaluated the coupling against the default GEB model outputs by simulating a portion of the Ghod Sub-basin in Maharashtra, India. We further explored various afforestation scenarios using the GEB-PlantFATE coupling with two levels of tree species diversity as represented by species richness (low and high biodiversity scenarios with 1 and 10 species, respectively).

We show that GEB-PlantFATE significantly improved the representation of feedbacks between the forests and hydrology with respect to the individual models alone. Our results show that the coupled model is able to better represent the changing species composition, NPP and size distribution under a changing hydrological and climatological environment, and the feedback from drought-adapted forest species to soil moisture. Forests simulated in GEB-PlantFATE could maintain photosynthesis under lower soil water content with respect to GEB only, and optimise photosynthesis better when higher water content was available.

https://doi.org/10.5194/egusphere-2026-5313
Preprint. Discussion started: 9 November 2026
© Author(s) 2026. CC BY 4.0 License.



Accordingly, we found two relatively high-water tolerant species as being the most successful in the high biodiversity scenarios. Finally, afforestation generally increased soil water content, with high biodiversity having a larger effect, likely due toindividual trees size.Overall, differences in NPP and transpiration rate between the high and low biodiversity scenarios could be primarily attributed to the faster growth rate of the low biodiversity species. The coupling represents a first step towards investigating forest biodiversity and eco-hydrological interactions in a hydrological model. We demonstrate the coupling on a relatively small basin, but the model can be applied to other regions to evaluate trade-offs between afforestation, forest use, and other water demands. This work indicates the potential that the coupled GEB-PlantFATE can more accurately simulate the advantages and disadvantages of afforestation, and the impact of climate change on the ecohydrological system.

1 Introduction

As our climate changes, we will be confronted with increasing extreme events, such as droughts and floods (Calvin et al., 2023). Water stress in particular is predicted to be more severe in a growing number of regions due to increased water demand for agricultural, domestic and industrial water use, a warmer climate with longer periods of low precipitation (Kummu et al., 2016; Schewe et al., 2014) and reduced natural aquifer recharge (Berghuijs et al., 2024). This combined overexploitation and lack of recharge is leading to a global depletion of groundwater resources (Wada et al., 2010). Water conservation projects across the globe seek to mitigate these issues, for which they require accurate predictions of the hydrological cycle. Afforestation, or planting forests in areas previously without tree cover, can be an attractive nature-based solution (NBS) to reduce droughts (Bussotti and Pollastrini, 2025; Gupta et al., 2024; Verheyen et al., 2024) and floods (Dittrich et al., 2019), while providing several ecosystem services (or co-benefits) such as timber production, cooling during heatwaves, CO_2 sequestration, and habitat for species important to local populations (Debele et al., 2023).

Forests can dramatically influence the water cycle, both positively and negatively. For example, forests can increase soil moisture by forming healthy soils, increasing infiltration and enhancing water retention (Moos et al., 2018; Rüegg et al., 2022). Moreover, canopies can reduce soil evaporation (Ilstedt et al., 2016; Jones et al., 2020). However, water losses from increased transpiration and rainfall interception evaporation can also lead to an overall decrease in soil moisture, groundwater levels, and stream flow (Jackson et al., 2005; Khorchani et al., 2021; Stavi et al., 2024). While uncertainties are large and the strength of the aforementioned processes can be highly dependent on the local climate and environment, afforestation is often suggested as an effective nature-based solution to water scarcity in the long run (Kamble et al., 2025).

Conversely, forests are also affected by the water cycle; species' hydraulic properties will affect forest composition on adaptation to drought (Anderegg et al., 2020). Drought stress in trees can cause embolisms, i.e. the formation of air pockets in the xylem that break the water column and prevent water from reaching organs for crucial functions (Choat et al., 2012; McDowell, 2011; McDowell et al., 2022). Embolisms can cause significant tissue damage in trees and, in extreme cases, lead to the death of the tree. To combat water stress, trees may acclimate to local conditions by adjusting their photosynthetic apparatus to maximize carbon gain while minimizing water loss (Franklin et al., 2023). Some trees may close their stomata or drop their leaves during drought to prevent water loss and potential embolism (Vico et al., 2015). In the long term, some species may become more resistant to embolism by evolving traits that increase their hydraulic safety margin during drought (McDowell et al., 2008). However, under changing conditions, strategies adapted to local water regimes may become maladaptive, leading to mass-drought extinction events, especially in locations that are not usually considered water-limited (Allen et al., 2010).

https://doi.org/10.5194/egusphere-2026-5313
Preprint. Discussion started: 9 November 2026
© Author(s) 2026. CC BY 4.0 License.

Distributed hydrological models allow simulation of water cycle processes over time across spatially varying domains by dividing the environment into grid cells typically ranging from 30' (~60 km at the equator) up to 30'' (~ 1 km at the equator) (Ai et al., 2020; de Bruijn et al., 2023; Burek et al., 2020). These models integrate various processes, including precipitation, soil water fluxes, discharge, and groundwater flow. Some of these models can simulate several distinct land-use types, including forests (de Bruijn et al., 2023; Burek et al., 2020; Sutanudjaja et al., 2018). In these models, the forest cover in each grid cell has its own vertical fluxes, including interception, evapotranspiration, and vegetation-specific transpiration (Sutanudjaja et al., 2018). However, vegetation is largely represented statically, and dynamic changes in species composition, age structure and local acclimation are generally not captured.

To better understand the bi-directional feedback between the water cycle and forest composition, several models that include both hydrology and vegetation dynamics have been developed. For example, the recently developed FORHYCS model (Speich et al., 2020) couples the existing PREVAH hydrological model (Gurtz et al., 1999) and the TreeMig forest landscape model (Lischke et al., 2006). The innovation of the FORHYCS model is that it simulates growth and mortality at the size-class level, accounting for successional dynamics and interspecific competition (Speich et al., 2020). However, it does not include species-specific responses to drought, nor does it model the acclimation of physiological processes in response to environmental conditions.

Therefore, we present a newly developed coupling of the Geographical, Environmental, and Behavioural (GEB) model (de Bruijn et al., 2023) with the Plant Functional Acclimation and Trait Evolution (PlantFATE) model (Joshi et al., 2023a). GEB is a coupled socio-hydrological model that combines an agent-based farm decision-making model (ABM) with an adapted version of the hydrological model CWatM (Burek et al., 2020). It can simulate both large-scale hydrological processes and the interactions (both responses and influences) of individual households and farmers with the hydrological cycle.

PlantFATE is a trait- and size-structured dynamic vegetation model that uses the P-hydro photosynthesis model (Joshi et al., 2022) and implements various eco-evolutionary processes, including light competition, vegetation demographics, and trait evolution. The advantage of using PlantFATE over other vegetation models is that, in addition to representing species-specific tree growth, mortality, and succession, it can also capture the short-term acclimation of photosynthesis and transpiration to water-stressed conditions using optimality theory, and over longer periods of time, the adaptation of traits to changing environmental conditions within an ecological, multi-species context.

In this work, we present a description and an example application of the GEB-PlantFATE coupling in the Ghod-subbasin, located in the Western Ghats and in the upper part of the major Krishna Basin in India. This area is increasingly impacted by droughts and lower groundwater tables (Surinaidu et al., 2013), and afforestation has been suggested as a potential solution to offset drought effects at the basin level, as well as provide other services such as carbon sequestration, timber production, and human well-being (Gupta et al., 2024). In this basin, tribal communities form a large part of the population and government programs such as the 2006 Indian Forest Rights Act (FRA) have been established to reassign ownership of areas to these communities, which have traditionally used the forest for their livelihoods pre-colonisation (Aggarwal, 2011; Lee and Wolf, 2018). Using the coupled model, we:

(i) Compare the coupled responses of forests and hydrology (simulated by coupling the GEB model with PlantFATE) with uncoupled GEB simulations;
(ii) Demonstrate the capability of the coupled model to simulate the impacts of afforestation on basin-wide hydrology in a future climate;

https://doi.org/10.5194/egusphere-2026-5313
Preprint. Discussion started: 9 November 2026
© Author(s) 2026. CC BY 4.0 License.

(iii) Compare the effects of planting a monoculture vs a diverse forest plantation on basin hydrology and carbon sequestration potential.

2 Model description

2.1 Source models

GEB (de Bruijn et al., 2023) is a coupled agent-based and hydrological model. It simulates a range of hydrological processes, including precipitation, discharge, and vertical fluxes (i.e., infiltration and percolation), over space and time at a daily timestep. Each 30'' grid cell (~1 km at the equator) is subdivided into smaller, dynamically sized hydrological response units (HRUs). Each HRU represents a single land use type, such as forest or land owned by an individual farming household. These HRUs allow the simulation of "vertical" hydrological processes, such as land-use (incl. forests) specific transpiration, although transpiration is currently represented only with pre-defined parameters using a crop factor. In addition, it uses crop group numbers (de Wit et al., 2020), where higher crop group numbers indicate a higher drought resistance. Crop group numbers for forests are obtained from LISFLOOD (Van Der Knijff et al., 2010). Hereafter, we refer to this as "simplified transpiration". In addition, the grid cells (containing one or more HRUs) are horizontally connected through the groundwater (simulated with MODFLOW) and river routing using the kinematic wave approach. GEB has previously been used to simulate the response to water stress of 12.1 million farmers in the Krishna basin of India, showing how irrigation and crop choice can influence the basin-wide hydrological system and vice versa. The full description of the GEB model is provided in de Bruijn et al. (2023) and Kalthof et al. (2025).

The PlantFATE model simulates forest establishment and demographics (growth, mortality, and seed production) in a single patch. It is designed to model how forest ecosystems adapt to climate change over multiple timescales, based on eco-evolutionary principles. It is spatially scale-independent and can be run at a custom timestep, as processes are aggregated to the desired temporal resolution. To align with the GEB model, we used a daily timestep for this study. The model employs a physiologically structured population modelling (PSPM) approach using the libpspm solver (Joshi et al., 2023b) and is both size- and trait-structured, meaning that the population is represented by cohorts of different sizes and species represented by variations in their plant functional traits. The size-based structure accounts for growth-stage-specific population dynamics and competition for light, whereas trait structure allows the species community to change in response to environmental changes.

Short-term processes: In the short term (i.e. here daily), PlantFATE implements CO_2 assimilation, respiration, growth, and other crucial plant processes. To account for the acclimation of photosynthesis, PlantFATE uses the P-hydro photosynthesis model, which maximizes CO_2 assimilation based on hydraulic traits, and environmental conditions, such as temperature, CO_2, vapor pressure deficit, and soil water potential (Joshi et al., 2022). Since P-hydro explicitly represents plant water balance and optimal stomatal responses to water stress, it is particularly suited for coupling with hydrological models.

Medium-term processes: In the medium term (i.e., yearly), species composition in PlantFATE is driven by light competition and other demographic dynamics such as growth, mortality and establishment.

Long-term processes: Finally, in the long term (i.e., decades to centuries), eco-evolutionary dynamics operate: populations can be invaded by randomly generated species, while species already present in the environment can shift their functional trait distributions via evolutionary dynamics, capturing the ascent of species towards fitness peaks.

PlantFATE is forced with five environmental inputs (i.e., temperature, light intensity, vapor pressure deficit, soil moisture and CO_2 concentration) to forecast the dynamics of multi-species communities, forest structure, and trait distributions over time.

https://doi.org/10.5194/egusphere-2026-5313
Preprint. Discussion started: 9 November 2026
© Author(s) 2026. CC BY 4.0 License.

PlantFATE has previously been used to accurately predict multiple emergent ecosystem properties characterizing forest structure and function in the Amazon Forest, as well as to predict shifts in community composition in response to elevated CO_2 (Joshi et al., 2023a). A full mathematical description of the Plant-FATE and P-hydro models is provided in Joshi et al. (2023a) and Joshi et al. (2022).

2.2 Coupling of the models

In the coupled model, each individual forest HRU in GEB is linked with an instance of the PlantFATE model, resulting in a total of 135 PlantFATE instances in the case-study region. The beginning of each daily timestep in GEB proceeds as default until the soil module. Here, for each forest HRU, GEB communicates with the relevant PlantFATE instance, exchanging variables related to soil water and transpiration. These include soil water potential, vapor pressure deficit, photosynthetic photon flux density, temperature, volumetric water content, and net radiation. PlantFATE then uses this information to update the forest state (see below) and calculate transpiration. This transpiration is communicated back to GEB, and transpired water is removed from the soil water storage (Fig. 1a and b).

The soil water potential, ψ, is calculated from soil moisture content, θ, wilting point, field capacity, and thickness, as described by Landsberg and Sands (2011).

$$\psi = -a_{\psi}\theta^{-n_{\psi}}, \quad (1)$$

Where a_{ψ} and n_{ψ} are positive parameters based on the wilting point and field capacity of the soil.

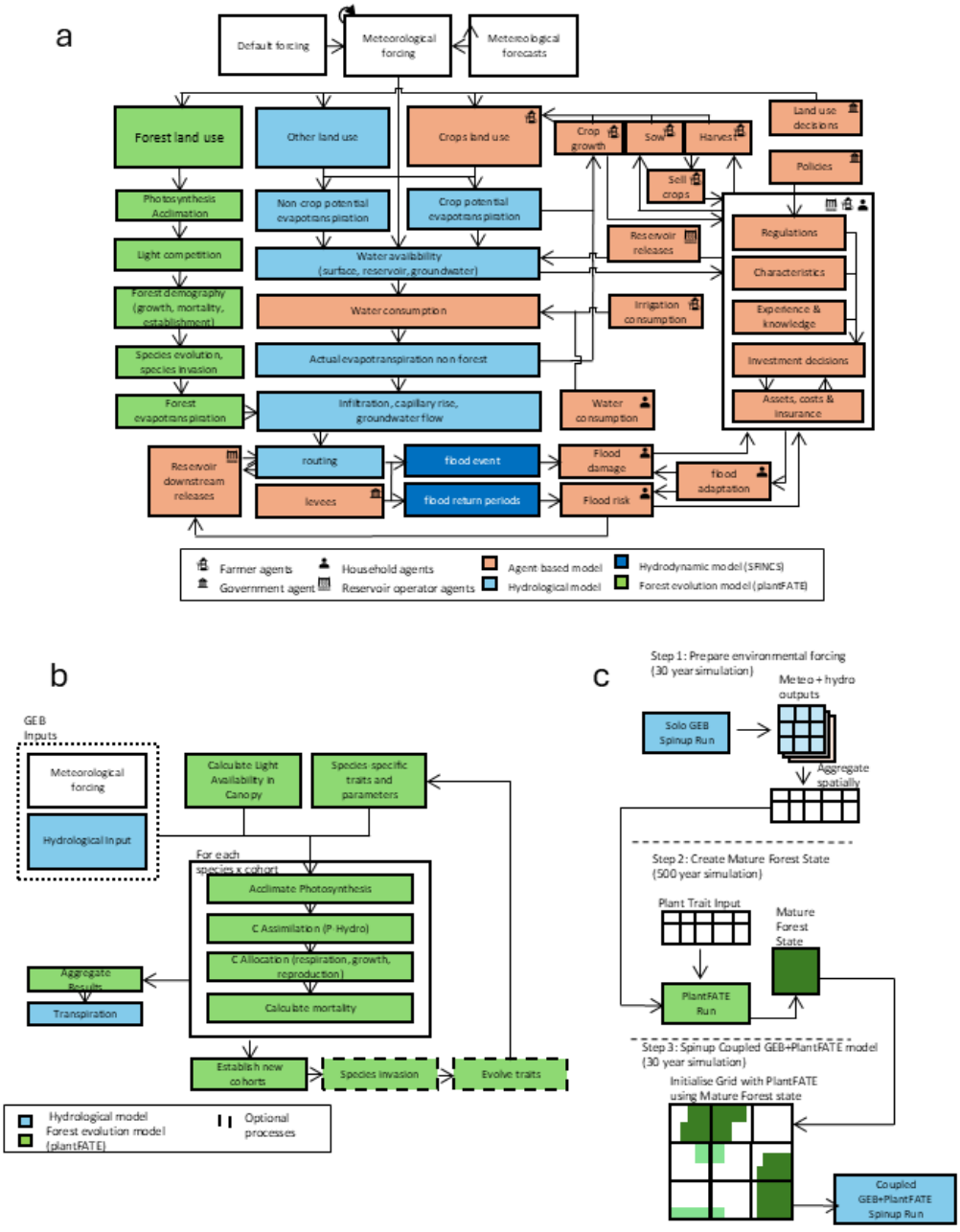
Vapor pressure deficit is calculated from temperature and relative humidity using the method of Buck, (1981). The atmospheric inputs to PlantFATE are either passed directly from the forcing data used in GEB, ensuring alignment with the hydrological simulations, or are calculated after minor common atmospheric calculations. PlantFATE then performs all *short-term processes* (e.g., photosynthesis, growth, and mortality) for each species-cohort combination. Cumulative transpiration is then returned to GEB to calculate the remaining water balance in the HRU and the grid cell.

In addition, the *medium- and long-term processes* in PlantFATE are performed at annual or larger timesteps. This includes adding new cohorts once a year to represent the establishment of seedlings and invasion dynamics, in which a new species is introduced to the community every 50 years.

Because an HRU can have a dynamic size, some forests and their associated HRUs only cover a very small percentage of a grid cell (e.g., a row of trees). To limit the computational demands of these small HRUs, we used PlantFATE only in grid cells with at least 25% forest cover, applying the GEB-default Penman-Monteith transpiration to all remaining cells with lower forest cover. In addition to the existing forest, the user can supply a map of new afforestation areas, which will be initialized during a new run. In this case, we did not limit PlantFATE use based on a minimum area threshold, as young forests have fewer cohorts and are thus less computationally demanding. Therefore, all these newly afforested areas become Forest HRUs with a PlantFATE instance upon the start of the run. This implies that a grid cell can contain more than one PlantFATE instances with forests of different ages. Currently, the coupling allows one set of species to be used as input for mature PlantFATE instances and another for afforestation PlantFATE instances. While unrealistic to have only these two possible compositions in a larger basin, this simplification is acceptable on a smaller scale, such as the study region used in this study.

Note that for other non-forest land-use types, transpiration is calculated using the simplified model already implemented in GEB.

https://doi.org/10.5194/egusphere-2026-5313
Preprint. Discussion started: 9 November 2026
© Author(s) 2026. CC BY 4.0 License.



185 **Figure 1 a) Schematic overview of the coupled GEB-PlantFATE model; b) Detailed schematic of PlantFATE, including meteorological forcing and hydrological model integration; c) Schematic for the derivation of mature PlantFATE instance parameters. In green processes, processes represented in PlantFATE are captured. In light blue, processes run by the CWatM-derived hydrological model module are captured. In orange, the agent-based model is captured; finally, in dark blue, the hydrodynamics model (SFINCS) is captured (not used in this study).**

https://doi.org/10.5194/egusphere-2026-5313
Preprint. Discussion started: 9 November 2026
© Author(s) 2026. CC BY 4.0 License.

2.3 Coupling Set-up

A PlantFATE instance can be started as a bare patch for the newly planted forest or initiated with a more mature forest for locations where forest already exists. To obtain parameters for mature forests, we run a separate "spinup" process involving several steps (Fig. 1c). We first run GEB without PlantFATE over a 30-year simulation period to obtain basin-wide climate and hydrology. The resulting climatic and hydrological data are then averaged across the basin and used together with local plant trait data as input to a PlantFATE-only run. Here, in step 2, a single PlantFATE instance, starting as a bare patch, is run independently of GEB for at least 500 years with a timestep of approximately 15 days and using average environmental conditions from across the basin. This results in a mature forest patch. Finally, in step 3, the final state from the previous PlantFATE outputs is used to initiate a mature forest in each PlantFATE patch in the coupled GEB-PlantFATE model and run for 30 years. This process allows each forest patch to acclimate independently to local conditions consistent with coupled hydrology. In this work, step 3 is not run long enough to capture variations in species composition across the basin, consistent with the purpose of the current study. This is sufficient for the current application which focuses on short-term impacts. In cases where spatial species variation and local adaptation are critical, the coupled spin-up can be run for longer (~5000 years) to allow vegetation to independently adapt to climatic conditions of each PlantFATE instance using the evolution setting of the PlantFATE model. Since this was not the objective of this study we had not done this at this instance. Once the initialization is completed, the coupled model can be used for each simulation of interest.

2.4 Technical implementation

GEB is implemented in Python, while PlantFATE is a C++ native application. Therefore, a Python interface for PlantFATE (py-pFATE) was developed using the pybind11 library (Jakob et al., 2017). This exposes PlantFATE to GEB and allows direct in-memory communication between GEB and multiple PlantFATE instances. The interface allows for multi-core parallel processing.

3 Model application

To demonstrate the use of the model, we applied it to a part of the Ghod subbasin, a 628km^2 area in the Pune District, Maharashtra, western India (Kanade et al., 2023). The Ghod subbasin is part of the Upper Bhima basin, which in turn lies within the heavily managed Krishna basin. The Ghod river originates in the Western Ghats at 1090 m above sea level and flows eastward for *c.* 200 km before joining the Bhima river. The climate of the region is sub-tropical, ranging from semi-arid to sub-humid, with most rainfall (circa 85%) coming from the South-West monsoon (June to mid-October). Rain is more abundant closer to the Western Ghats and decreases towards the southeast (Kanade et al., 2023; Rajguru and Kulkarni, 2018). The forested area in the Ghod subbasin is mostly confined in the northern Western Ghats (Kanade et al. 2023), where our study area is located (Fig. 2). Currently, 18% of the examined area is forested. Like the rest of the Upper Bhima basin, the focus area has a complex socio-ecological system related to water resources and land management (Kanade et al., 2023). There is a strong demand for water resources to irrigate crops, as the basin is important for agricultural production. Still, it is also increasingly exposed to floods, droughts and declining groundwater levels (Surinaidu et al., 2013). There is an interest in increasing the forested areas to 1) mitigate the negative effects of drought on basin-wide water availability, and 2) create a biodiverse forest to provide for forest-dependent tribal communities in the area (Kanade et al., 2023). An additional 18% of the subbasin area (118 km^2) could be returned to tribal communities under the Indian Forest Rights Act. In parts of these areas (Fig.2a, purple regions), referred to hereafter as FRA areas, could potentially be

https://doi.org/10.5194/egusphere-2026-5313
Preprint. Discussion started: 9 November 2026
© Author(s) 2026. CC BY 4.0 License.

used for afforestation or forest restoration, in consultation with local stakeholders. These regions were obtained from the Maharashtra Forest Department, Government of India in 2023.

To explore afforestation dynamics and identify trade-offs between biomass production and forest water use under future climate conditions, we used the coupled GEB-PlantFATE model across various afforestation scenarios in this area.

For this purpose, we created 3 model setups:

(i) GEB-PlantFATE with low biodiversity (1 species)
(ii) GEB-PlantFATE with high biodiversity (10 species)
(iii) GEB without PlantFATE

For the first two model setups we run six afforestation scenarios over the period 2020-2049 (with a spin-up period of 1990-2020). These areas correspond to 0, 20, 40, 60, 80 and 100% of the total potential FRA areas, and are randomly selected from the total potential area for afforestation (Fig. A1). For each afforestation scenario, the two model setups explore two cases of low and high biodiversity to investigate how species richness affects the forest resilience. For GEB without PlantFATE, only the unforested scenario was run. Combining the three model setups and biodiversity cases, this resulted in a total of 12 scenarios simulated.

https://doi.org/10.5194/egusphere-2026-5313
Preprint. Discussion started: 9 November 2026
© Author(s) 2026. CC BY 4.0 License.

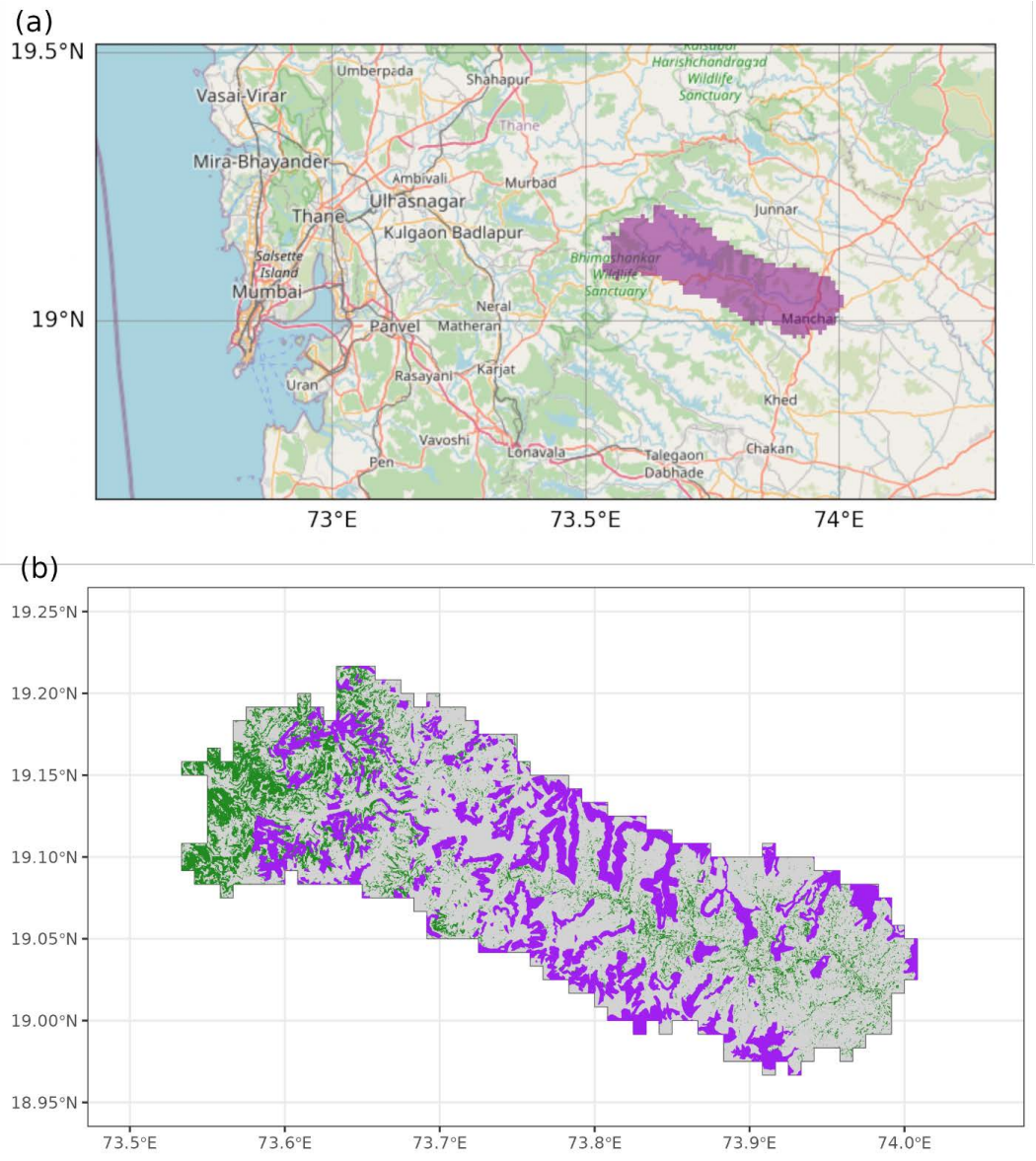


Figure 2 Map of the simulated part of the Ghod subbasin. (a) The region is located east of Mumbai, India, within the Northern Western Ghats. Map data © OpenStreetMap contributors. (b) The dark green spots represent locations of current forests, and the purple areas are pre-selected regions for potential afforestation (FRA areas).

3.1 Input data

To implement GEB hydrology in the Ghod subbasin, reservoir data were obtained from the HydroLAKES dataset (Messager et al., 2016), and land use was obtained from ESA WorldCover 2021 at 10 m resolution, downscaled to 1.5″ and mapped to GEB land use types. Forcing data was obtained from ISIMIP 3b (Frieler et al., 2024) for the SSP3-7.0 scenario from the GFDL-ESM4 general circulation model. SSP3-7.0 is characterized by moderate warming and medium-to-high greenhouse gas emissions, driven by strong regional rivalries worldwide. We used the historical and scenario-specific projections of CO_2 concentration (Meinshausen

https://doi.org/10.5194/egusphere-2026-5313
Preprint. Discussion started: 9 November 2026
© Author(s) 2026. CC BY 4.0 License.

et al., 2020) to run the third step of the model initialization and the coupled model runs. Soil data (e.g., percentages of sand, silt, and clay) were obtained from the SoilGrids dataset (Poggio et al., 2021) and used to derive hydrological variables such as saturated hydraulic conductivity and porosity (Rawls and Brakensiek, 1989). For other inputs, we refer to the model documentation (de Bruijn et al., 2025).

PlantFATE requires species-specific input on the following plant functional traits: wood density (ρ), the xylem pressure inducing 50% loss of hydraulic conductivity (P50), maximum height (H_{max}), and leaf mass per area (LMA). We used the ten most abundant species present in a study conducted nearby in the Bhimashankar Wildlife Sanctuary (Jezeera, 2016), as this satisfied the trade-off between species representation and plant trait data requirements. The P50 value for each species was found either from a nearby site (Sunny, 2020) or from a global database of P50 values generated using phylogenetic relationships between species (Knighton et al., 2025). The remaining traits for each species were obtained from the TRY Database (Kattge et al., 2020) and other databases or publications where necessary (see Table A1 for a full citation list). For other plant-related parameters, PlantFATE's default values were used.

3.2 Initialization

To initialize the coupled model, the three steps described in Section 2.3 (Fig.1c) were followed. In the first step, the GEB model initialization was run on its own using climate data for the period of 1960-1990. Then, using the environmental outputs from GEB, a synthetic 500-year climate data set was generated by first spatially averaging the mean monthly climatic data across the domain and then randomly resampling the 30 years of climate data. Using this synthetic climate data and the plant trait data for the locally most abundant tree species (according to Sunny, 2020, Fig. A2), a single instance of PlantFATE was run for 500 years, to obtain the establishment of a steady multi-species forest with invasion dynamics allowed. In the third step, the PlantFATE saved state data from the previous run was used as the starting point for PlantFATE instances in the coupled GEB-PlantFATE initialization. The third step was run for the 1990-2020 period, using atmospheric CO_2 from the SSP3-7.0 scenario (Meinshausen et al., 2020). The second and third steps were used to generate highly biodiverse, established forests to use as a starting point to simulate the afforestation scenarios in both low and high biodiversity cases. For the high biodiversity case, the same multi-species list used for the initialization was used for the new forest patches in all afforestation simulation. For the low biodiversity scenarios, newly afforested areas used a different species list with only a single species, which was taken to be the pioneer, fast-growing species *Aglaia lawii*, which dominated the initial 200 years of the steady multi-species forest from step 2 (Fig. A3). In these cases, *A. lawii* was initialised at a similar density as the combined density of the high biodiversity species.

4 Results

Forest photosynthetic response in the model is primarily driven by soil moisture, vapour pressure deficit (VPD), irradiation and temperature. As expected, we observe that when considering the yearly cycle, net primary productivity (NPP) was highest during the March-June period, at the start of the monsoon season, coinciding with the period with the highest temperature and with the highest irradiation (Fig. A4).

https://doi.org/10.5194/egusphere-2026-5313
Preprint. Discussion started: 9 November 2026
© Author(s) 2026. CC BY 4.0 License.

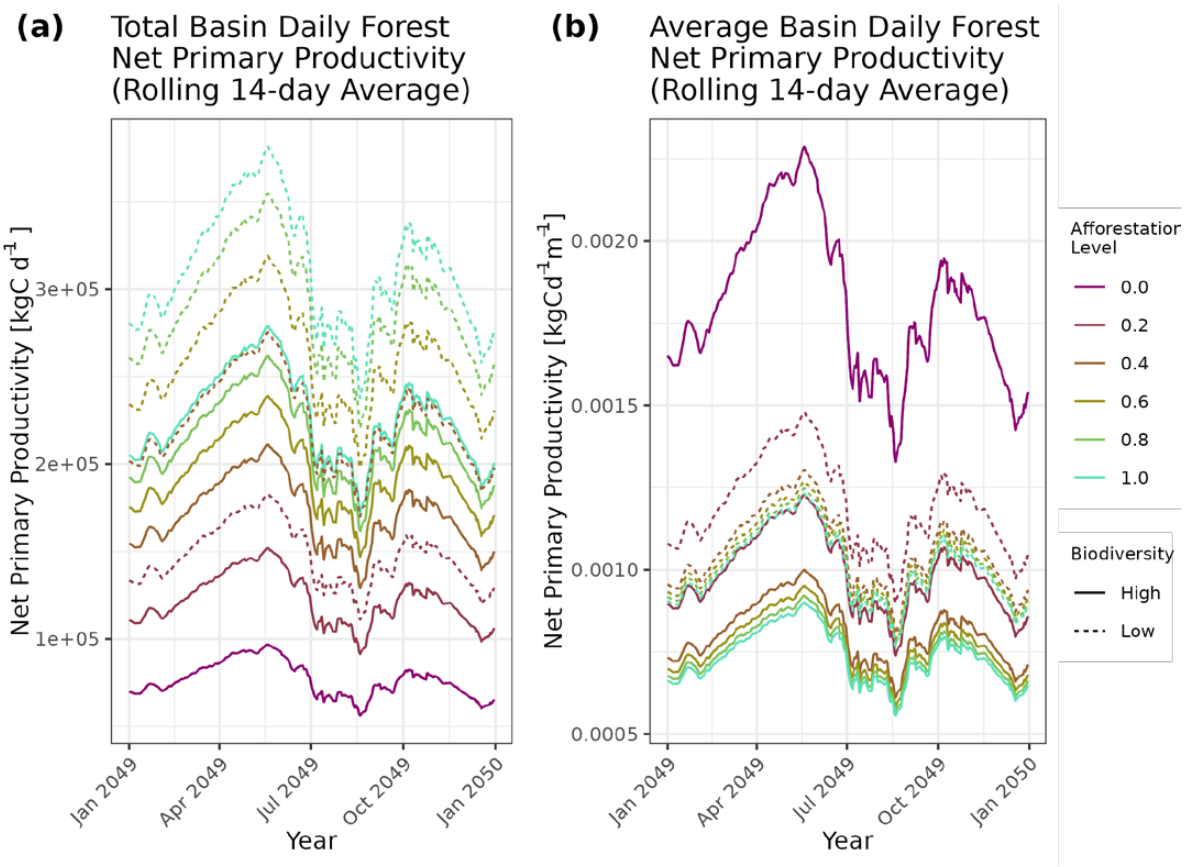


Figure 3 Total and average basin daily forest net primary productivity (NPP) in 2049. (a) Total daily NPP summed across the basin in 2049; and (b) average daily forest NPP, calculated across the basin in 2049. In both (a) and (b), values are smoothed by averaging over a 14-day period. Colours indicate the level of afforestation, continuous line indicate the high biodiversity case (10 spp.) and the dashed line the low biodiversity case (1 spp.). Note: the default GEB model formulation does not produce NPP outputs.

The basin had significantly higher soil moisture in the northwest part, which corresponds to the most mountainous region with higher rainfall and afforestation (Fig. A5). Correspondingly, transpiration was also higher in those regions and exhibited a clear seasonal cycle, as expected for the Bhima basin's monsoon-driven climate (Fig. A6).

4.1 Comparing model formulations

We compared the two model formulations (default GEB and GEB-PlantFATE) in a non-afforested scenario and examined water dynamics in the basin's forest grid cells throughout the runs. When examining normalised soil water content, default GEB showed higher soil moisture values in the lower-range, while GEB-PlantFATE consistently simulated higher values in the mid-range. At high soil moisture levels, both models performed similarly (Fig. 4a). Groundwater recharge and transpiration showed greater variability, with no clear patterns between the runs (Fig. 4b and c). Groundwater recharge showed greater disagreement closer to zero, where most points are clustered, while transpiration reached higher maximum values in GEB than in GEB-PlantFATE, which exhibited a narrower range. When averaged across the basin, we found marginally higher soil moisture in the GEB-PlantFATE for all values (Fig. 5a), no discernible difference in groundwater recharge (Fig. 5b) and higher transpiration in the default GEB model for higher value range and in GEB-PlantFATE for lower transpiration value range (Fig. 5c). The differences between the runs can be primarily identified in the northwest part of the basin, which is also the wettest, with GEB-PlantFATE consistently showing

https://doi.org/10.5194/egusphere-2026-5313
Preprint. Discussion started: 9 November 2026
© Author(s) 2026. CC BY 4.0 License.

higher moisture content, especially under drier conditions (March and June), while months following the higher precipitation from the monsoon season (June-August) appeared more homogeneous between runs (Fig. 6).

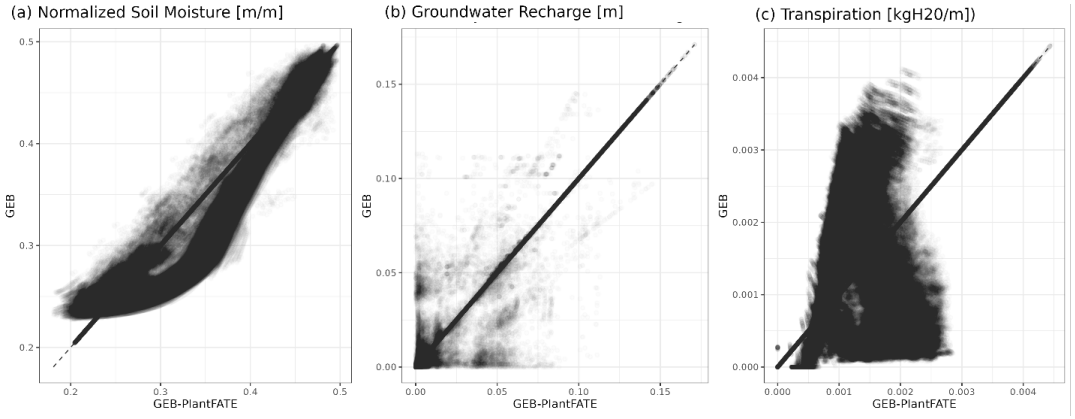


Figure 4 Comparison between default GEB and GEB-PlantFATE model formulations across the basin throughout 2031-2049 years of the simulation for a) normalized soil moisture, b) groundwater recharge and c) forest transpiration. Each point represents a single cell and time step (day), considering forest cells only. The dashed line is a one-to-one line. Points falling exactly on the one-to-one line are cells where forests occupy <25% and, therefore, PlantFATE is not used.

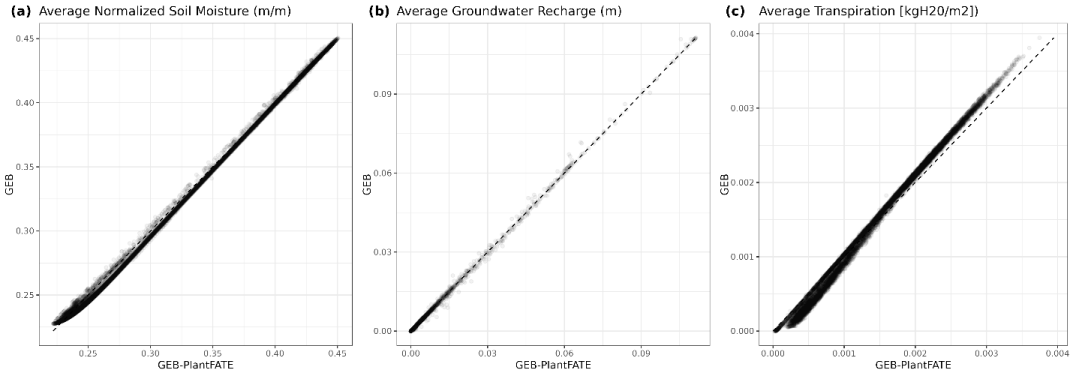
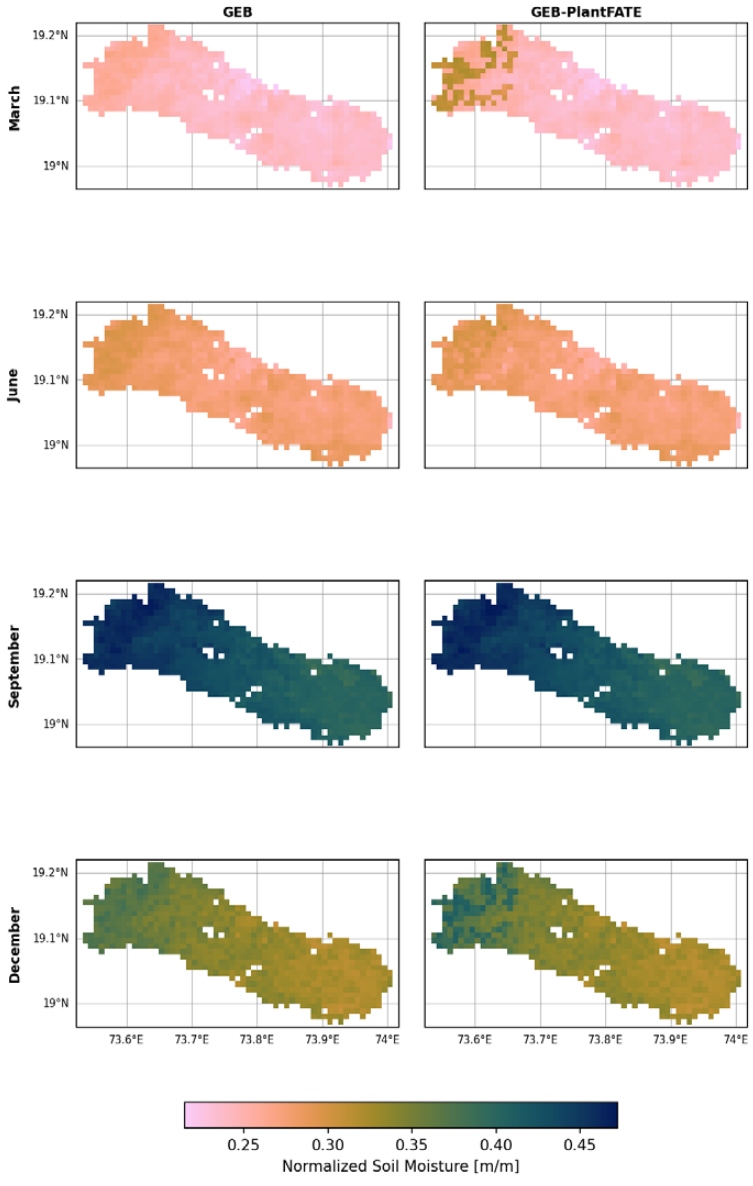


Figure 5 Comparison between default GEB and GEB-PlantFATE model formulations across the basin throughout 2031-2049 years of the simulation for average a) normalized soil moisture, b) groundwater recharge and c) forest transpiration. Each point represents a basin average value across all forest cells for a single time step, considering only forest cells. The dashed line is a one-to-one line.

https://doi.org/10.5194/egusphere-2026-5313
Preprint. Discussion started: 9 November 2026
© Author(s) 2026. CC BY 4.0 License.



310

Figure 6. Basin map showing averaged monthly soil moisture content (m) in the default GEB (left column) and GEB-PlantFATE (right column) runs. The results from four months are presented to show the yearly seasonality between wet and dry seasons.

4.2 Effects of afforestation

Afforestation led to higher yearly average soil moisture in forested cells (Fig. 7a) and, to a lesser extent, in the entire basin (Fig. 315 A5). When comparing within a year, soil moisture differed significantly primarily in the driest periods of the year, whereas during the monsoon season, soil moisture remained similar between different afforestation levels (Fig. 7b).

https://doi.org/10.5194/egusphere-2026-5313
Preprint. Discussion started: 9 November 2026
© Author(s) 2026. CC BY 4.0 License.

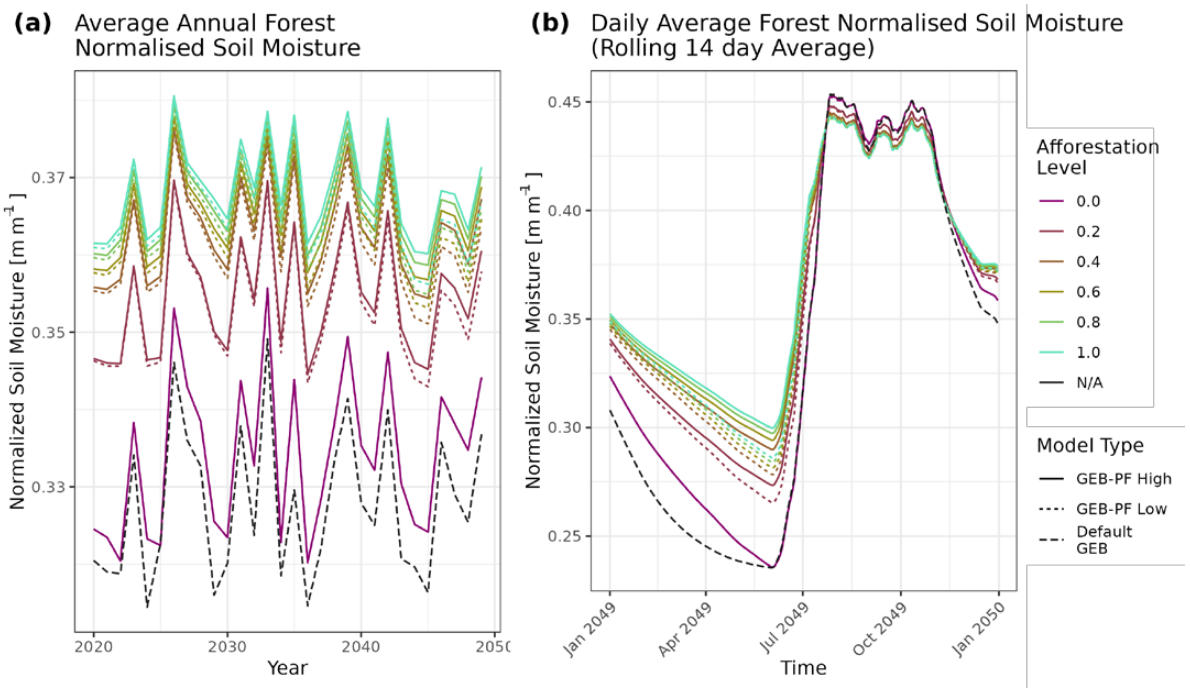


Figure 7 a) Average annual soil moisture in forest cells across the Ghod Sub-basin over the entire simulation period and b) rolling (14-day) average soil moisture (mm^{-1}), averaged spatially across the forest cells in the Ghod Sub-basin in 2049, the last year of the simulation. In each scenario, only forest cells (both preexisting and newly afforested) are represented, and therefore, with increasing afforestation, the average accounts for increasingly larger forest areas. Colors indicate the level of afforestation, and continuous and small dashed lines correspond to the high (10 ssp.) and low (1 ssp.) biodiversity cases, respectively. The long-dashed line indicates the default GEB run.

As expected, with forest growth, the total transpiration generally increased over the course of the simulation (Fig. 8a) as afforested areas expand, with higher afforestation levels showing a stronger increase in total forest transpiration. However, when looking at the average transpiration per unit area (m^2), average forest transpiration appeared to be lower in higher afforested scenarios, probably reflecting the lower contribution to total transpiration of newly afforested areas compared to established forests (Fig. 8b).

https://doi.org/10.5194/egusphere-2026-5313
Preprint. Discussion started: 9 November 2026
© Author(s) 2026. CC BY 4.0 License.

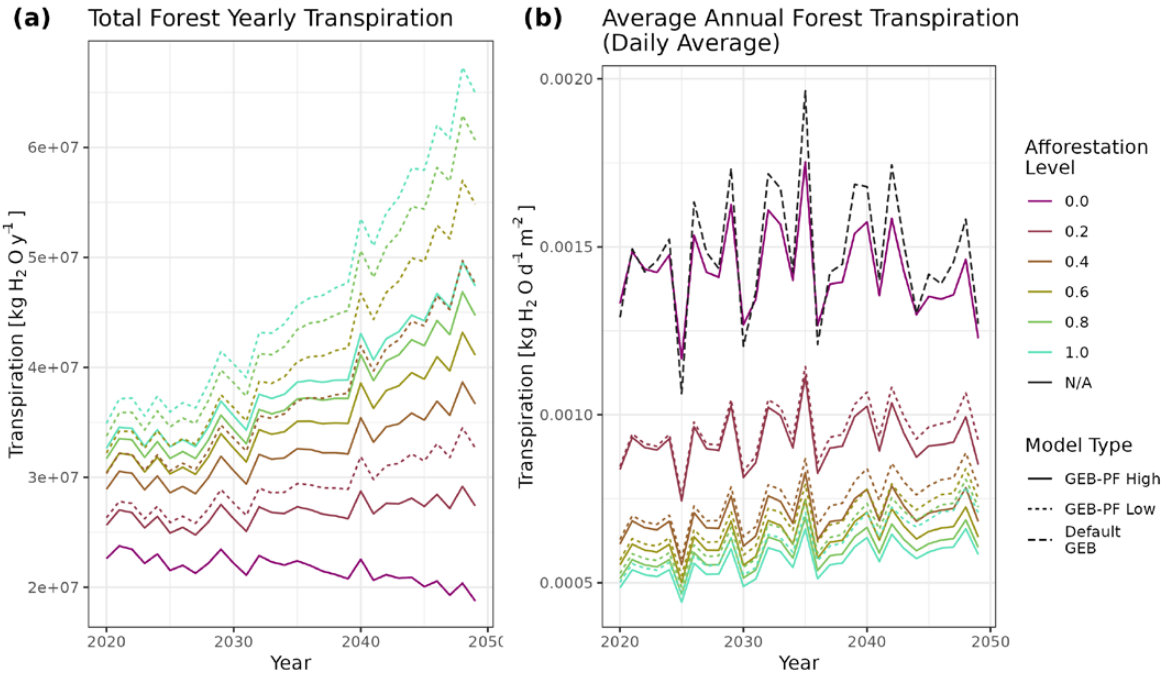


Figure 8 a) Total forest transpiration per year. b) Average daily transpiration per m2 in a single year. Colors indicate the level of afforestation, and continuous and small dashed lines correspond to the high (10 spp.) and low (1 spp.) biodiversity cases, respectively. The long-dashed line indicates the default GEB run.

4.3 Biodiversity effects

GEB-PlantFate runs with scenarios of high biodiversity (10 species) and low biodiversity (1 species) showed variable responses in the immature, newly afforested cells for photosynthesis and subsequently, for biomass. NPP was higher under low biodiversity (Fig. 9a), which resulted in more growth and biomass accumulation over the simulation period, except in the lowest afforestation scenario (Fig. 9b). Accordingly, also transpiration levels were higher for less biodiverse afforestation scenarios than for higher biodiverse ones (Fig. 8a and b). Simultaneously, soil water moisture was higher in the higher biodiversity scenarios (Fig. 7a).

We also found, after investigating a random subset of PlantFATE instances across the basin (Fig. A8), that species composition within PlantFATE changed over time in newly afforested areas for high biodiversity scenarios (A10). In the low biodiversity runs, we used only the pioneer species for afforestation, the fast-growing *A. lawii* (Fig. A11). Mortality rate in the new forests was higher for low biodiversity than for high biodiversity (Fig. A12), potentially due to differences in biomass rather than competition or

https://doi.org/10.5194/egusphere-2026-5313
Preprint. Discussion started: 9 November 2026
© Author(s) 2026. CC BY 4.0 License.

water stress. In contrast, in existing, mature forests species appear to have occasionally experienced larger water stress, as indicated by very negative soil water potential, which led to higher mortality rates (Fig. A13).

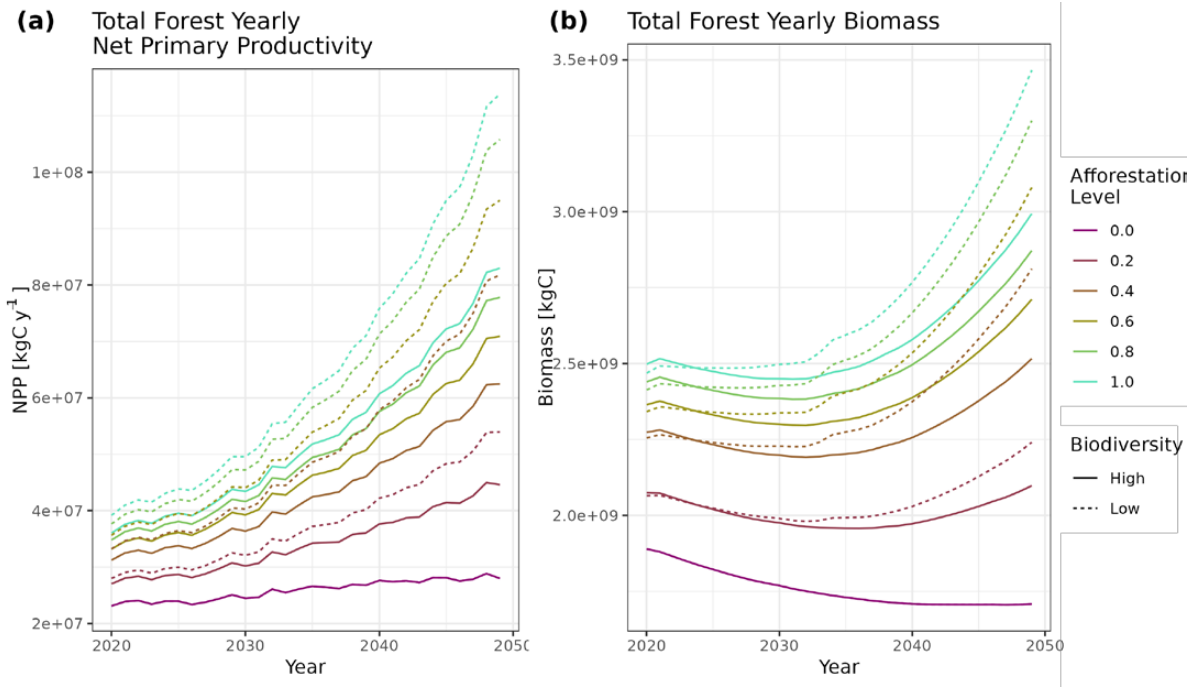


Figure 9 Total forest yearly NPP and biomass in the GEB-PlantFATE simulations. a) Total NPP over each year in the GEB-PlantFATE simulations for the forest cells. b) Total biomass over each year in the GEB-PlantFATE simulations for the forest cells.. Colors indicate the level of afforestation in the different scenarios, and line type represents biodiversity cases> continuous line indicates high biodiversity (10 species), and dashed line indicates low biodiversity (1 species).

5 Discussion

In this paper, we present a coupling between a dynamic hydrological model and a dynamic vegetation model capable of investigating the effects of different forest composition, age, and structure on basin-wide hydrology. We apply the coupled model to investigate varying levels of afforestation and species composition in the Ghod subbasin of the Upper Bhima Basin. Below, we outline how the coupling performed against the default GEB model formulation, afforestation and biodiversity effects and discuss limitations and possible improvements on the models.

5.1 Comparison to the existing forest model

Our application to the Ghod subbasin of the coupled model revealed differences in water dynamics, as indicated by soil moisture content, and to a lesser extent by transpiration, between the default GEB and GEB-PlantFATE models formulation. In all runs, both transpiration and soil moisture follow a clear seasonal cycle with lower values during the drier months, and higher values in the period following the intense precipitation of the monsoon season (June-August). Differences between GEB and PlantFATE-enabled versions were generally more evident under dry conditions and pre-monsoon months (between March and June), with PlantFATE forested areas maintaining higher transpiration and higher soil moisture content in comparison with default GEB forests. On the contrary, in wet monsoon months, when soil moisture is higher, transpiration in PlantFATE forested areas appears lower

https://doi.org/10.5194/egusphere-2026-5313
Preprint. Discussion started: 9 November 2026
© Author(s) 2026. CC BY 4.0 License.

than that of default vegetation. Overall, GEB-PlantFATE forests display lower interannual variability in soil water moisture and transpiration. Taken together, these results suggest a higher water use efficiency of the GEB-PlantFATE simulated forests compared to the default GEB forests throughout the simulation. A higher water used efficiency has been suggested to enhance forest resilience and alleviate the effects of water extremes, especially drought (Hu et al., 2022; Zhang et al., 2024).

This result might be because PlantFATE uses an optimisation-based approach to model photosynthesis of forests based on hydraulic traits. In contrast, in GEB, the much simpler approach with static crop group numbers (de Wit et al., 2020) is used. Because of this, the GEB-PlantFATE is able to simulate the ability of drought-tolerant species to photosynthesise under lower soil moisture values, including the change in species composition over time. Notably, the most drought-resistant species, *Garcinia talbotii* as indicated by its highly negative P50 value (i.e., the xylem pressure corresponding to 50% loss of conductivity; see Table A1), was the most abundant species in the basin in mature forest cells at the end of the simulations with *Aglaia Lawaii* second. The capacity to capture drought resistance in tree speciescan explain the higher photosynthesis (and so higher transpiration) under lower water availability of forests in the GEB-PlantFATE run, and optimisation-based photosynthesis may explain the higher efficiency of photosynthesis (and therefore less transpiration) in high water availability scenarios.

5.2 Effects of afforestation

In the afforestation simulations, even scenarios with just 20% of the suitable areas afforested were associated with higher average soil moisture, primarily in forested areas but also across the entire basin. Not unexpectedly, differences were more evident during the drier months, when water is scarcer, and lower or negligible during the monsoon season, when basin-wide water availability increases. Also total forest transpiration showed an increase with expansion of area afforested, due to the presence of more forest surface, but showed a decrease in average transpiration per unit area, likely due to the lower transpiration rates of younger trees in the newly afforested areas with respect to older and more mature forest patches.

Capturing variable forest composition and age along with species' traits is crucial in examining the response of forests to drought and its effect on water availability. Water use efficiency changes throughout forest age (Delzon and Loustau, 2005; Skubel et al., 2015), and younger forests generally have higher soil moisture than older ones because they are not yet established (Rabbai et al., 2023). Simultaneously, older forests may retain more rainfall due to more conducive soil properties (Ren et al., 2025). While our results show that younger forest did indeed have higher soil moisture and lower transpiration, we are currently unable to fully explore age dynamics in our model, due to the lack of a mechanism for capturing soil organic carbon and the associated water dynamics (see also **5.4 Limitations** below).

Afforestation and reforestation are popular strategies to increase carbon sequestration and lower the country's carbon emissions. Moreover, these strategies can have significant effects on local water dynamics, with decreased runoff and increased evapotranspiration, though their effects are less pronounced at the regional and national scale (Trabucco et al., 2008). Our results show that even small, afforested areas can improve basin-wide soil water availability. In India, afforestation has been shown to be an effective strategy, increasing water availability in agricultural areas and increasing yield (Kamble et al., 2025). Beyond water availability, afforestation and reforestation can increase downstream water quality (Keller and Fox, 2019) and potentially increase access to non-timber forest products crucial for local populations (Kanade et al., 2023; Lowore et al., 2018).

5.3 Effects of biodiversity

In the high biodiversity scenarios, the functional trait diversity of species led to variable growth rates and hydraulic resistance. In more mature forest cells, light competition and water availability resulted in some mortality and changes in forest composition in

https://doi.org/10.5194/egusphere-2026-5313
Preprint. Discussion started: 9 November 2026
© Author(s) 2026. CC BY 4.0 License.

both the initial PlantFATE spinup simulation and subsequent coupled model runs. Moreover, mature forests experienced more negative soil water potential compared to newly afforested areas, which indicates higher water stress. This led to increased mortality rates (Fig. A13), which might reflect the higher overall water use of more mature trees, although this association has not been explicitly tested.

In newly afforested areas, because of the short timescale of our simulations, we observed only limited competition among species, as this tends to occur after multiple decades. Nonetheless, we still observed some differences in species' biomass accumulation over the 30 years simulation; while the majority of the species increased their biomass (Fig. A10), others either remained constant (e.g., *Syzygium cumini* and *Mangifera indica*) or decreased it (*Syzygium gardneri)*. Overall, the lower biodiversity scenarios had higher photosynthesis and, therefore, overall higher growth than the high biodiversity scenarios. This result likely reflects the composition of new afforested area in the low biodiversity scenario, which are composed by only one fast growing species, *A. lawii*. Nevertheless, under the most afforested scenarios, NPP more than doubled for both the low and high biodiversity scenarios during the timescale of the simulation.

In general, results across biodiversity scenarios confirmed the previous observation that the ability to capture different species traits, as enabled by PlantFATE, is crucial to simulate the capacity of forests to respond to limited water availability. In both biodiversity scenarios, plants showed a higher capacity to photosynthesise in low-water conditions, which likely contributed to high photosynthesis in the pre-monsoon period when plants can take advantage of higher temperatures and radiation. However, in our afforestation simulations, we did not observe any instances of drought conditions that could led to high forest mortality, thus preventing us from comparing difference in capability to cope with drought conditions between the two biodiversity scenarios. However, previous papers showed that higher tree diversity can increase a forest's resilience or adaptive capacity to drought (Fajardo and Piper, 2021; Pretzsch et al., 2014; Sousa-Silva et al., 2018). This may be due to facilitation and complementarity of species (Haberstroh and Werner, 2022), as well as niche partitioning, allowing different species to use nutrients and water at different soil depths (Brassard et al., 2013; Richards et al., 2010). Further development of soil dynamics and other methods of capturing diversity of forest-water interactions in our model would help capture these effects in the future (see also **5.4 Limitations** below).

5.4 Limitations

In the non-afforested scenarios, we observed a decline in current forest biomass that stabilized towards the end of the simulation in 2050, as well as a loss of two species, changes that cannot be fully explained by climate changes and water dynamics. This suggests that the forest dynamics between the PlantFATE-only run and the final simulations might have not yet fully stabilized. However, our choice of the time frame (2020-2050) was limited by the need to align our simulations with the SSP scenario. In the future, with more data availability, this may be remedied with improvements on the initial spin-up operation, such as increasing the length of the spin-up period as well as running each cell separately. Such changes would also allow multiple forest compositions to be implemented in the run. However, these changes would need to be balanced with computational requirements of the model and further testing would be necessary to determine feasibility.

Beyond technical improvements, further work would be necessary to couple other integral processes relevant to forest-water interactions. For example, forests are positively associated with soil organic carbon (SOC), which, in turn, has long been documented to aid in water retention. Including SOC information improves the prediction of soil water characteristics (Rawls et al., 2003), and adequate SOC reduces runoff and soil erosion (Rugendo et al., 2023). Moreover, the relationship between forests and water retention is not static: mixed and older forests generally show higher levels of soil organic matter (Devi, 2021), and

https://doi.org/10.5194/egusphere-2026-5313
Preprint. Discussion started: 9 November 2026
© Author(s) 2026. CC BY 4.0 License.

conversion of primary forests to plantations or *secondary* forests is often associated with decreased soil organic carbon pool (Zhang et al., 2024). Extending the coupling to better represent the soil organic carbon accumulation and associated hydrological dynamics would greatly benefit the accurate representation of forest successional growth stages from secondary to old-growth forest stands.

Finally, in our model, we currently lack the capacity to capture storage of non-structural carbohydrates (NSC), which have been shown to maintain cell turgor and prevent water loss (Hesse et al., 2019) and thus would be required for improved tree drought response. Specifically, representing NSC and carbon storage in model simulations (Stefaniak et al., 2026c) may allow capturing climate seasonality by mechanistically representing forest survival in response to seasonal droughts.

6 Conclusion

In our study, we demonstrate a coupling of an agent-based hydrological model, GEB, with a dynamic vegetation model, PlantFATE, to examine the relationship between forest growth and catchment hydrology. We model a range of afforestation scenarios in a part of the Ghod Subbasin in the Upper Bhima Basin using a variable species-diversity scenario. By using a dynamic, optimisation-based and vegetation trait-based forest model, we can simulate forest development (including younger or older forest stands) and hydraulic responses over time, including adaptation to drought and water. Vice versa, we simulate how those forests affect drought and water availability.

We show that the coupled model decreases local water availability under low moisture conditions, likely due to a combination of species drought tolerance and higher transpiration, but increases it under high moisture conditions, likely because of improved representation of plant water-use efficiency. Together these two effects allow for smaller and more realistic year to year variations between soil moisture as compared to the default formulation and ultimately more water availability during the dry and pre-monsoon periods. Under scenarios of afforestation, higher afforestation increases forest soil moisture availability, likely due to lower forest water use in immature forest cells. High biodiversity scenarios had lower NPP and growth than the low biodiversity ones and therefore had higher soil moisture availability, though longer scenario runs would be needed to evaluate the subsequent effects of competition and self-shading in the new forests.

Further work will involve technical and scientific development of both PlantFATE and the coupled model. Capturing additional hydrologic responses, including non-structural carbohydrate storage to account for periods of low photosynthetic activity, would be crucial to account for more accurate representation of drought response. Moreover, soil organic carbon dynamics, which can significantly alter soil runoff and infiltration, are another avenue for exploring forest-hydrology relationships, especially as it may relate to flooding in addition to droughts. We also envision that in the future our coupled model can be used to further investigate trade-offs between afforestation, forest use, and agricultural demands, especially when the full functionality of the agent-based model, which simulates the behaviour of households and reservoir operators, is utilized.

Overall, our work shows that afforestation in the Ghod Subbasin can have a strong positive effect on soil water availability at the basin-scale, and that high tree diversity can increase tree biomass production. This is particularly important in a future climate when periods of drought are more likely to occur.

Appendix A Supplementary Figures and Tables

Table A1 Trait data used for PlantFATE tree species parameterisation. Values rounded to two decimal places (heights rounded to nearest metre, using the upper bound where a range was reported in the source). Superscript indicates the source of the value: a Kattge et al., 2011; Kattge et al., 2020 (TRY Plant Trait Database); b Knighton et al., 2025; c Chakrabarty & Balakrishnan, 1990; d Pati et al., 2022;

https://doi.org/10.5194/egusphere-2026-5313
Preprint. Discussion started: 9 November 2026
© Author(s) 2026. CC BY 4.0 License.

e Sunny, 2020; f Flowers of India (accessed 30 June 2025); g Bally, 2006; h Green, 2003; i Singh et al., 2019; j Zanne et al., 2009 (Global Wood Density Database); k Tropical Plants Database, Ken Fern (accessed 30 June 2025); l eFlora of India (accessed 30 June 2025); m Manohan et al., 2023

Species Name	Wood density $\rho\ [gcm^{-3}]$	Xylem pressure corresponding to 50% loss of conductivity P50 $[MPa]$	Maximum Height $H_{max}\ [m]$	Leaf Mass per Area $LMA\ [gm^{-2}]$
Dimorphocalyx lawianus	0.72[a]	-1.78[b]	6[c]	65.84[a]
Memecylon umbellatum	0.64[d]	-1.61[e]	2[f]	140.07[a]
Mangifera indica	0.52[a]	-1.43[e]	30[g]	111.11[a]
Olea dioica	0.66[a]	-1.77[e]	15[h]	75.98[a]
Syzygium cumini	0.64[a]	-2,88[e]	30[i]	107.86[a]
Litsea stocksii	0.42[j]	-2.46[b]	20[k]	77.88[b]
Lepisanthes tetraphylla	0.81[a]	-2.40[b]	13[f]	140.75[a]
Garcinia talbotii	0.72[a]	-3.18[b]	20[f]	94.36[a]
Syzygium gardneri	0.73[a]	-1.85[b]	60[l]	61.98[a]
Aglaia lawii	0.64[a]	-2.70[b]	15[f]	60.00[m]

https://doi.org/10.5194/egusphere-2026-5313
Preprint. Discussion started: 9 November 2026
© Author(s) 2026. CC BY 4.0 License.

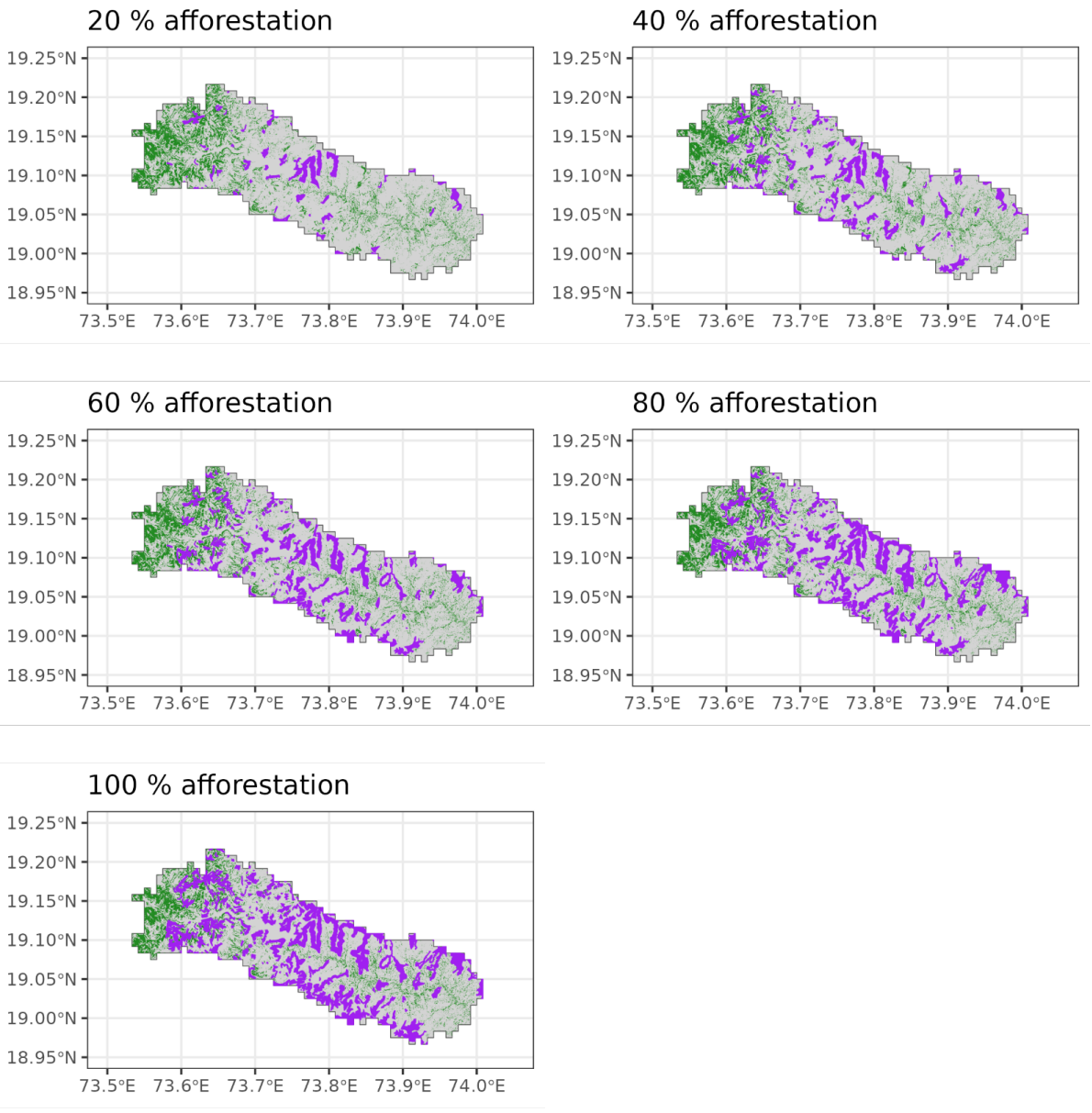
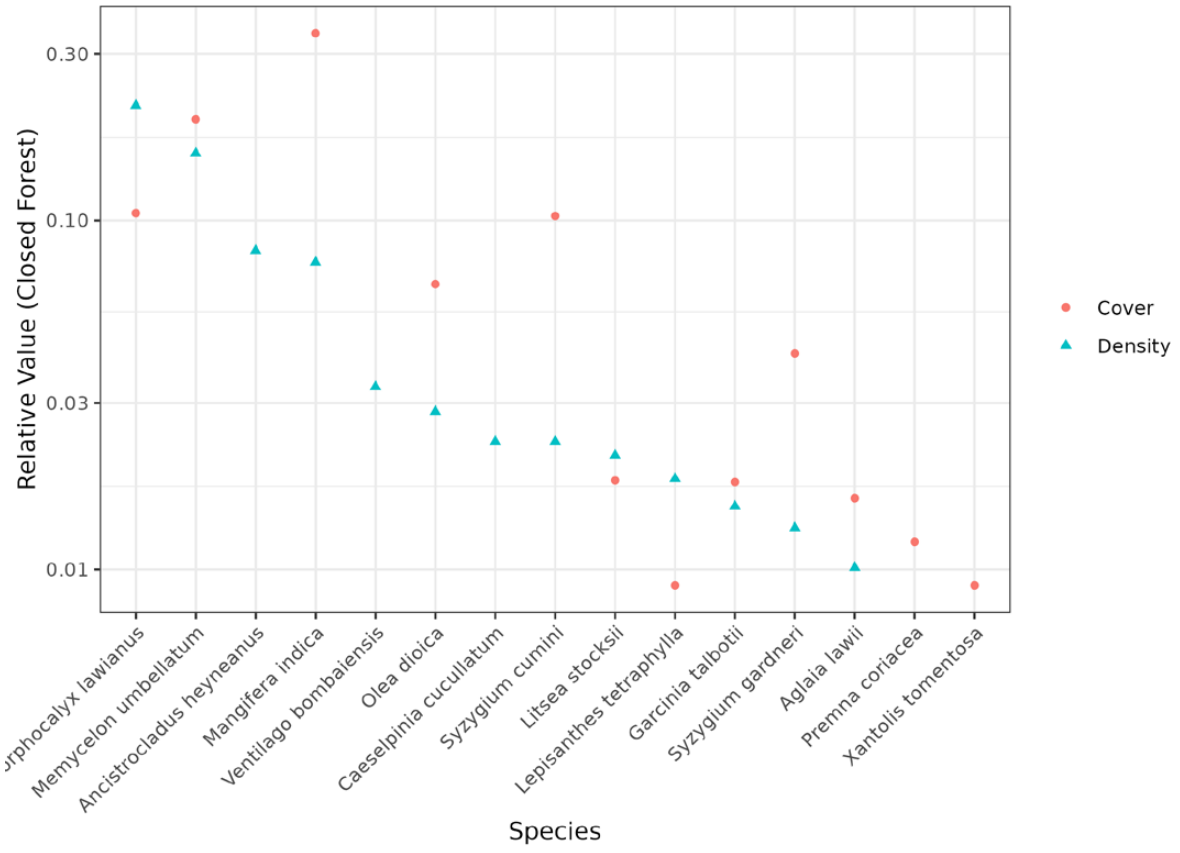


Figure A 1 Afforestation scenarios. Dark green areas are locations of existing forests. The purple polygons are the locations selected for each afforestation scenario, which increase sequentially.

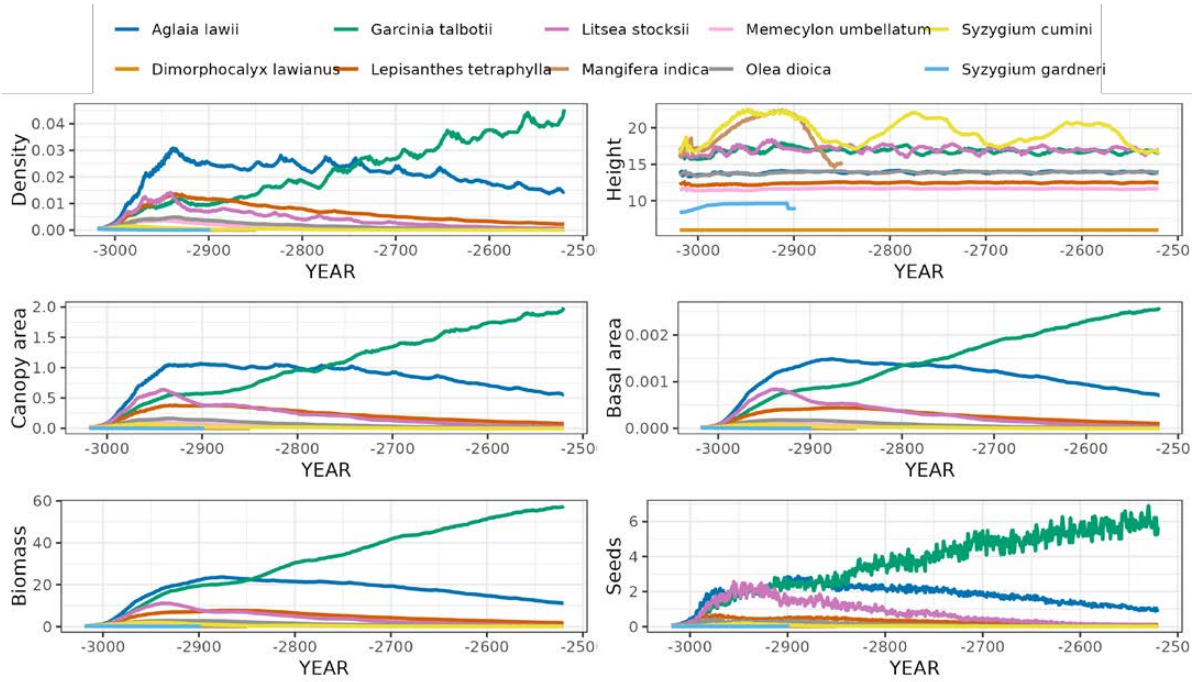
https://doi.org/10.5194/egusphere-2026-5313
Preprint. Discussion started: 9 November 2026
© Author(s) 2026. CC BY 4.0 License.



480

Figure A 2 Relative density and cover comparison (log10 scale) of tree species of the Northern Western Ghats, as reported by Jezeera (2016). A threshold value of 0.009 for both density and coverage was applied in order to include species in the present study. The 10 species with both relative density and coverage above 0.009 were selected for the high biodiversity scenario.

https://doi.org/10.5194/egusphere-2026-5313
Preprint. Discussion started: 9 November 2026
© Author(s) 2026. CC BY 4.0 License.



485 **Figure A 3 Species properties during the solo PlantFATE run to establish mature forest. Colours refer to individual species.**

https://doi.org/10.5194/egusphere-2026-5313
Preprint. Discussion started: 9 November 2026
© Author(s) 2026. CC BY 4.0 License.

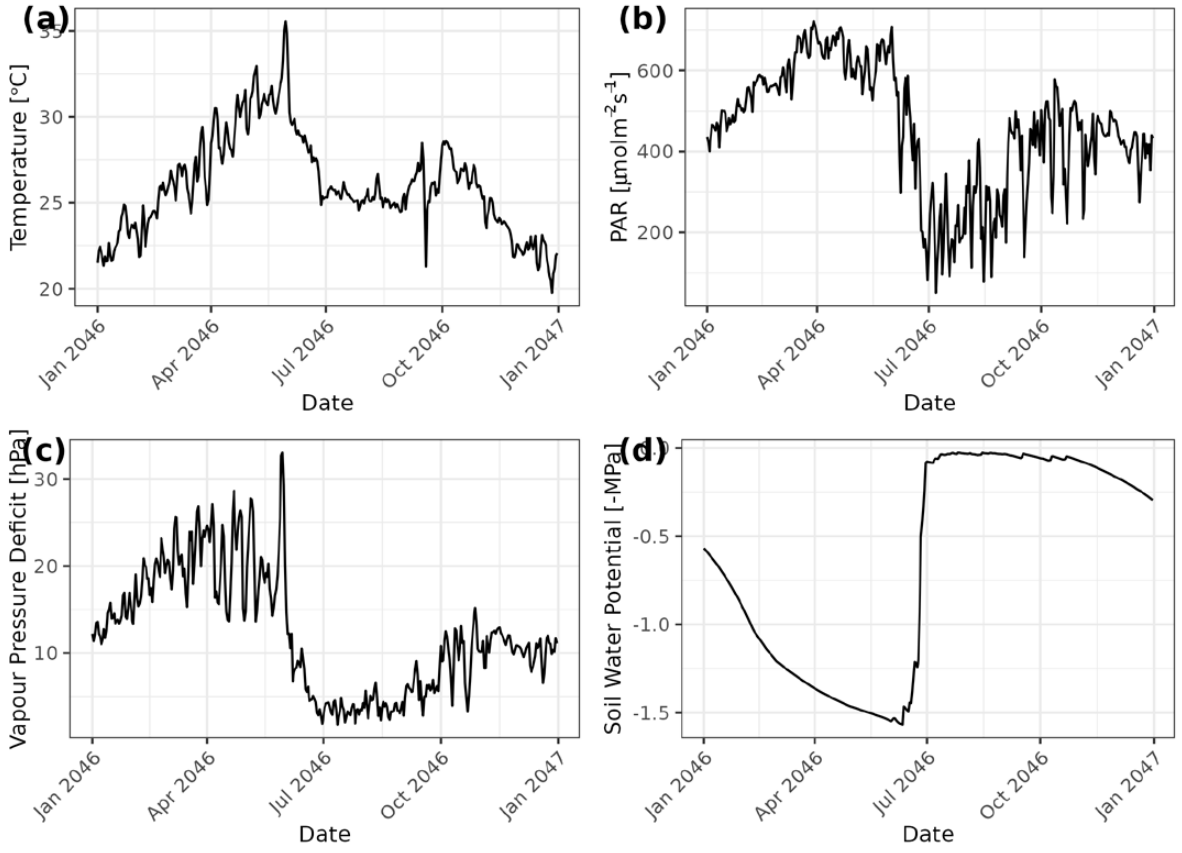
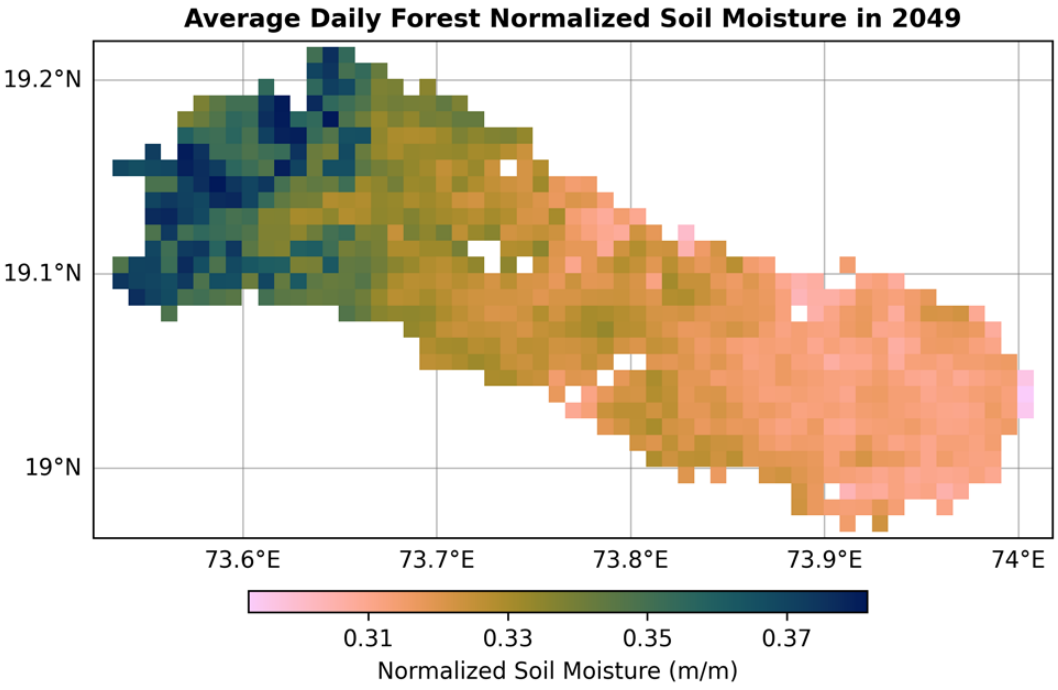


Figure A 4 Intraannual climatic and soil variables averaged across the basin for the year 2046. Temperature (a), photosynthetically active radiation (PAR, b), vapour pressure deficit (VPD, c) and soil water potential (d) are the primary climatic inputs to PlantFATE model driving tree responses.

https://doi.org/10.5194/egusphere-2026-5313
Preprint. Discussion started: 9 November 2026
© Author(s) 2026. CC BY 4.0 License.



490

Figure A 5 Average daily soil moisture in forest cells in 2049 (example result for GEB-PlantFATE with no afforestation and high biodiversity).

https://doi.org/10.5194/egusphere-2026-5313
Preprint. Discussion started: 9 November 2026
© Author(s) 2026. CC BY 4.0 License.

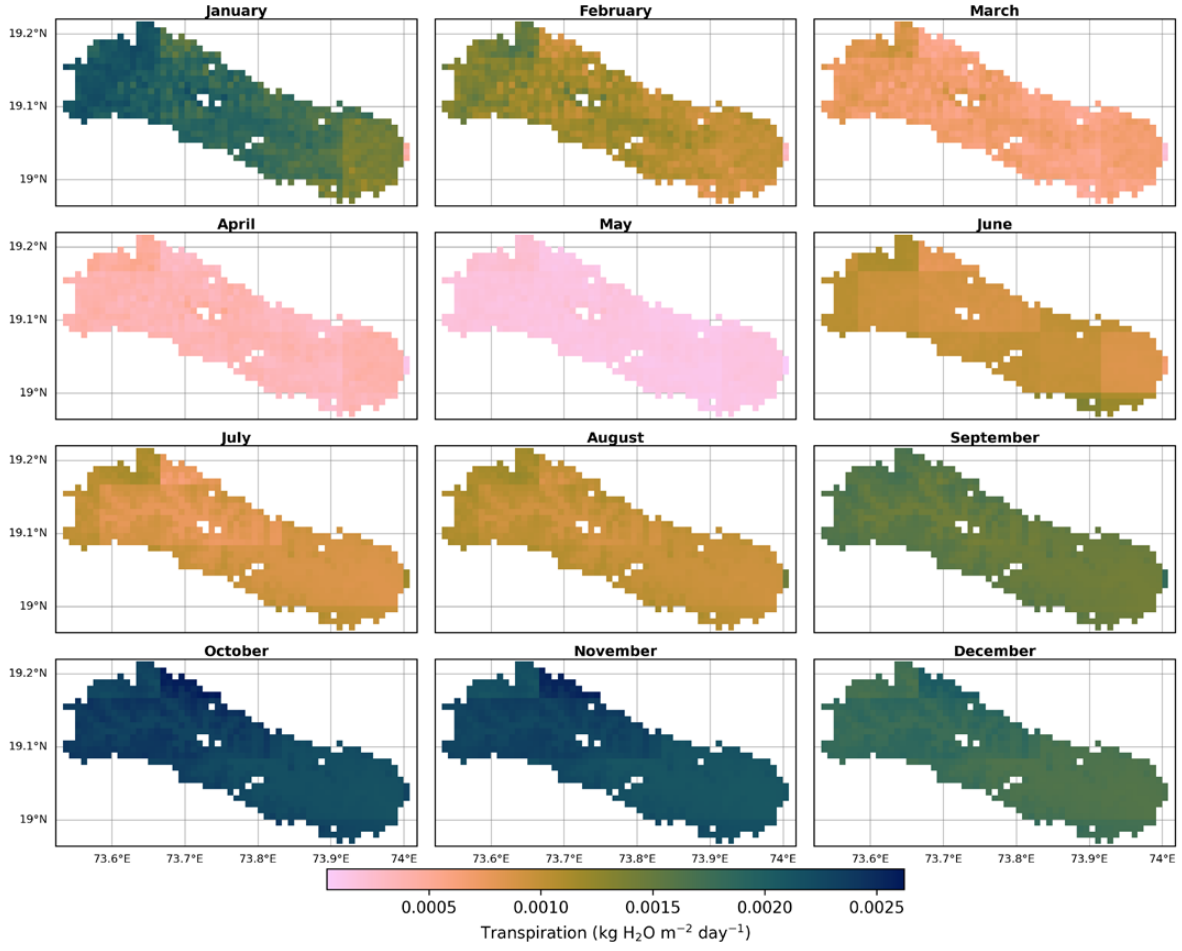


Figure A 6 Basin map showing the difference in the averaged monthly forest transpiration for the GEB only run

495

https://doi.org/10.5194/egusphere-2026-5313
Preprint. Discussion started: 9 November 2026
© Author(s) 2026. CC BY 4.0 License.

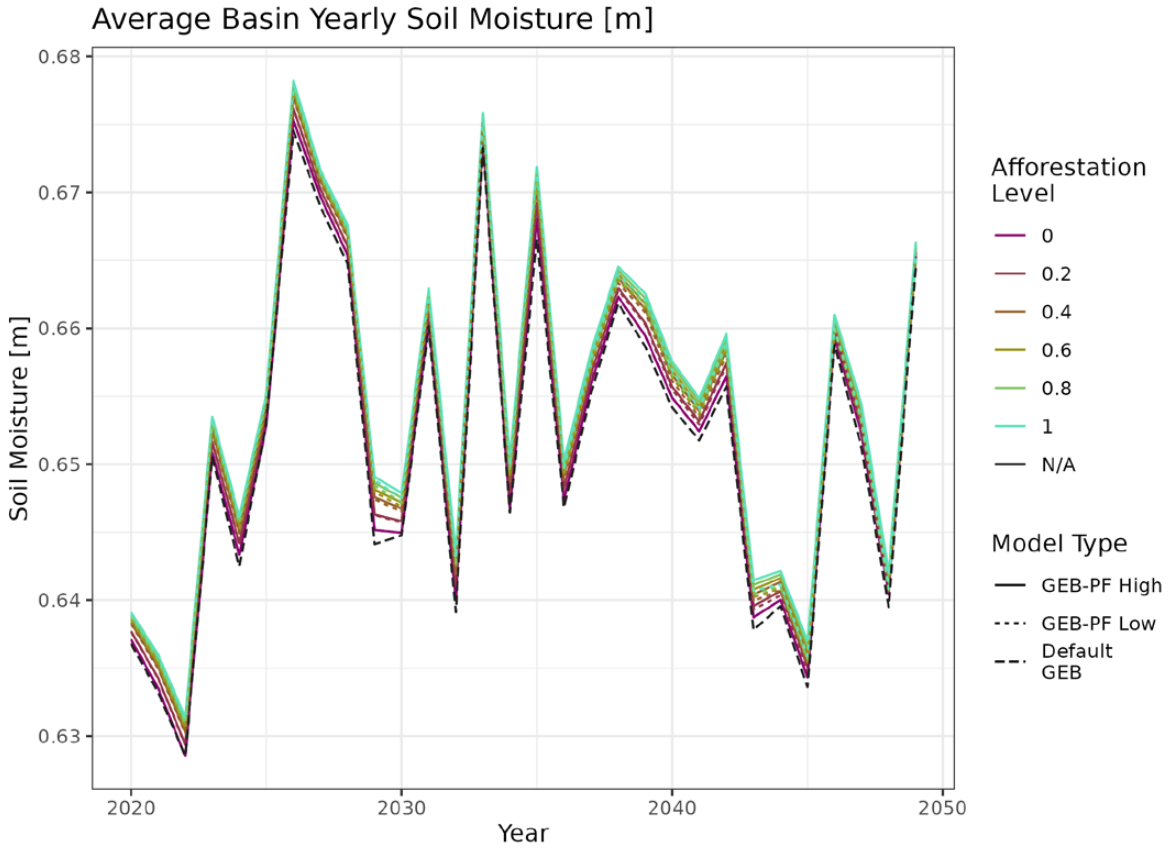


Figure A 7 Non-normalized soil moisture averaged across the entire basin (forest and non-forest areas). Colors indicate the level of afforestation, and lines correspond to the number of species (10 high biodiversity and 1 low biodiversity, no species in the default GEB formulation) modelled with PlantFATE.

https://doi.org/10.5194/egusphere-2026-5313
Preprint. Discussion started: 9 November 2026
© Author(s) 2026. CC BY 4.0 License.

500

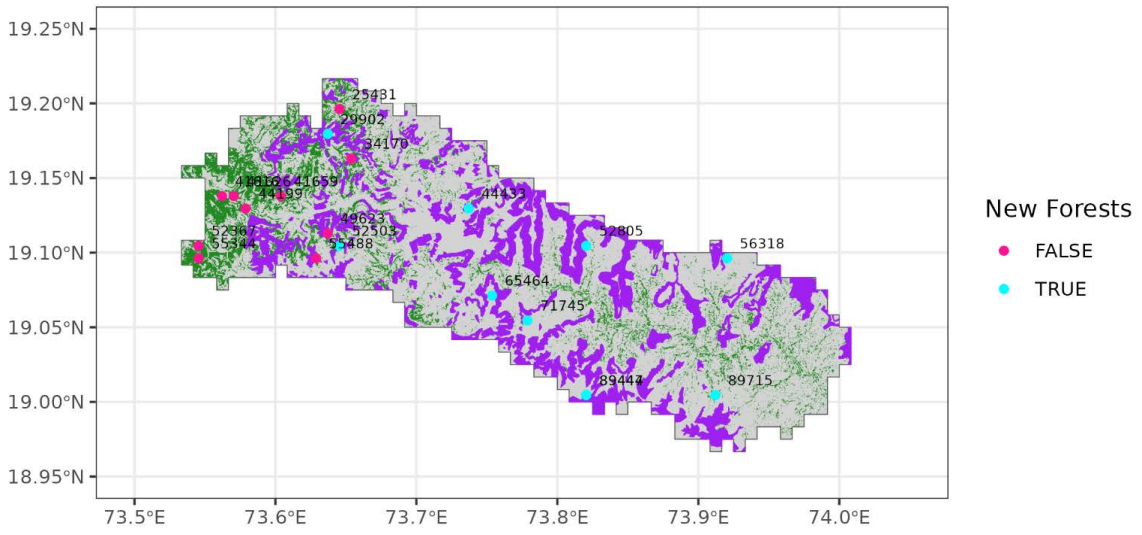


Figure A 8 Location of the 20 randomly selected PlantFATE forest cells used to explore forest growth dynamics in the highest afforestation scenario. Dark green areas are locations of existing forests. The purple polygons are the locations selected for each afforestation scenario, which increase sequentially. Pink dots are existing and, therefore, mature forest cells and blue dots are new forest cels.

505

https://doi.org/10.5194/egusphere-2026-5313
Preprint. Discussion started: 9 November 2026
© Author(s) 2026. CC BY 4.0 License.

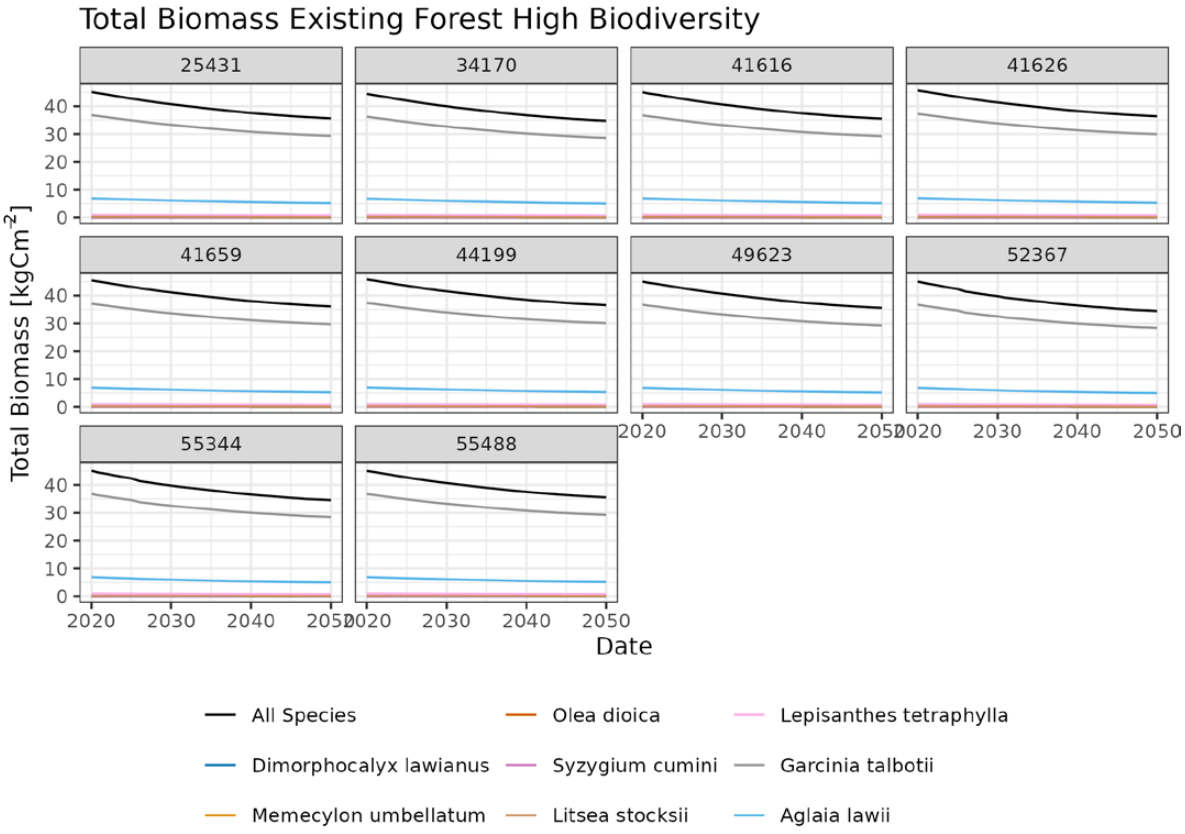


Figure A 9 Total biomass per unit area of individual species throughout the simulation in randomly selected cells representing mature forests. Colours refer to individual species. Black line indicates the total biomass for all species. Some of the original 10 species did not survive the spinup period.

https://doi.org/10.5194/egusphere-2026-5313
Preprint. Discussion started: 9 November 2026
© Author(s) 2026. CC BY 4.0 License.

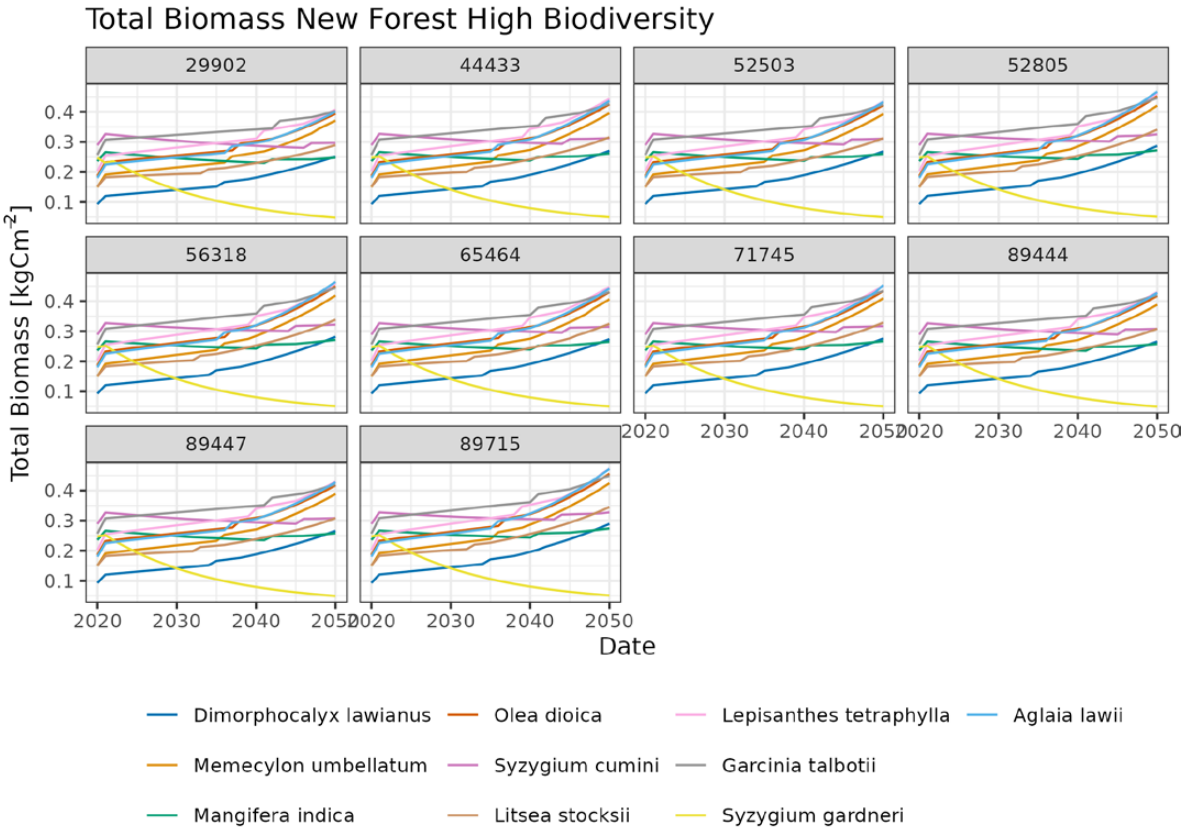


Figure A 10 Total biomass per unit area of individual species throughout the simulation in randomly selected cells of the high biomass, 100% afforestation scenario in new forest cells only. Colours refer to individual species.

https://doi.org/10.5194/egusphere-2026-5313
Preprint. Discussion started: 9 November 2026
© Author(s) 2026. CC BY 4.0 License.

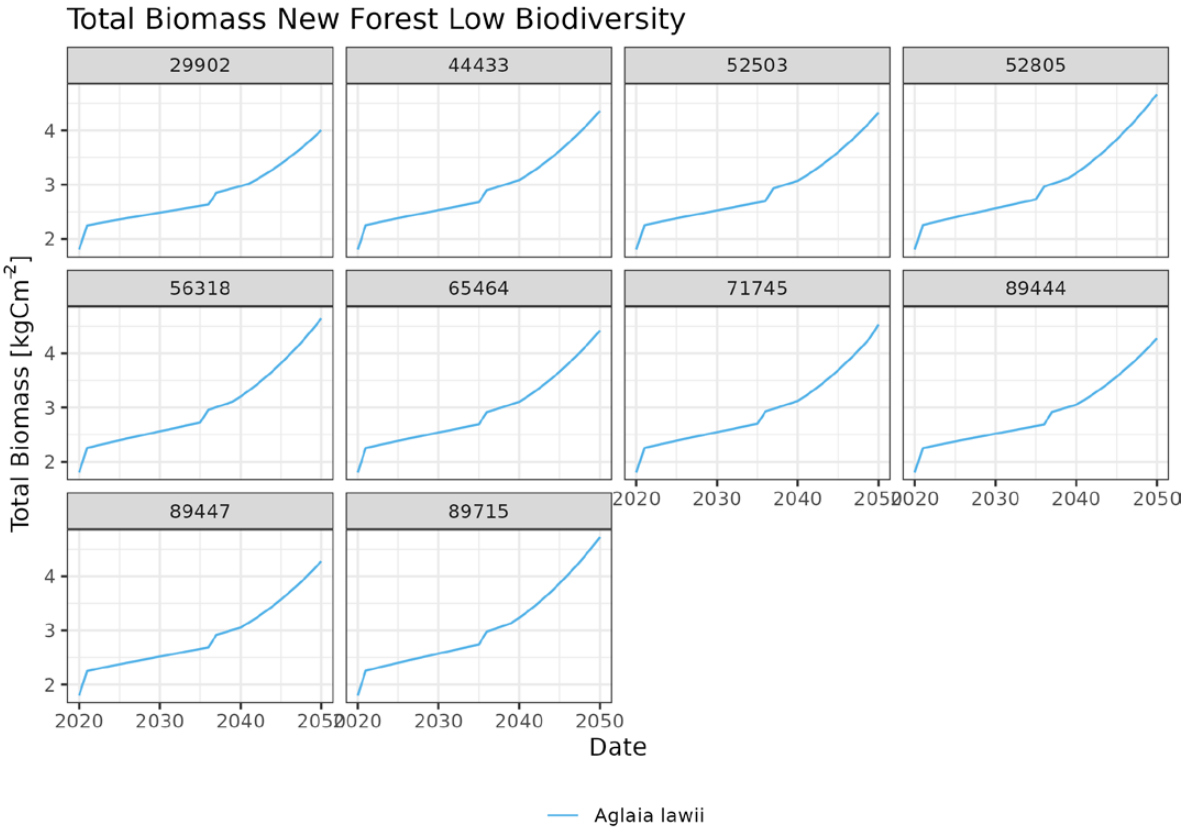
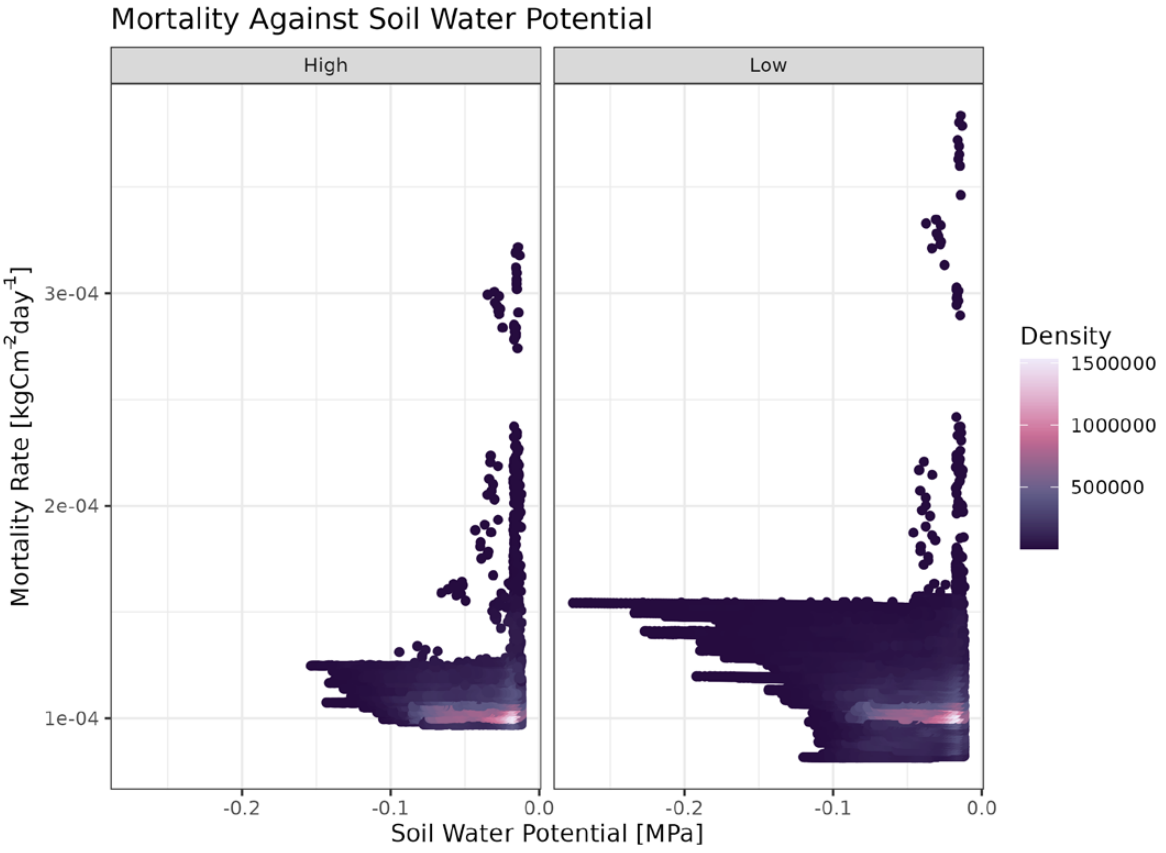


Figure A 11 Total biomass per unit area of individual species throughout the simulation in randomly selected cells of the low biomass, 100% afforestation scenario in new forest cells only.

https://doi.org/10.5194/egusphere-2026-5313
Preprint. Discussion started: 9 November 2026
© Author(s) 2026. CC BY 4.0 License.



520 **Figure A 12 Mortality rate under different soil water potential values throughout the simulation for randomly selected new forest cells (Fig A8) in the most afforested scenario for high biodiversity (left) and low biodiversity scenarios (right). More negative soil water potential indicates higher water stress. Color indicates kernel density with brighter colours indicative of more points in that part of the plot.**

https://doi.org/10.5194/egusphere-2026-5313
Preprint. Discussion started: 9 November 2026
© Author(s) 2026. CC BY 4.0 License.

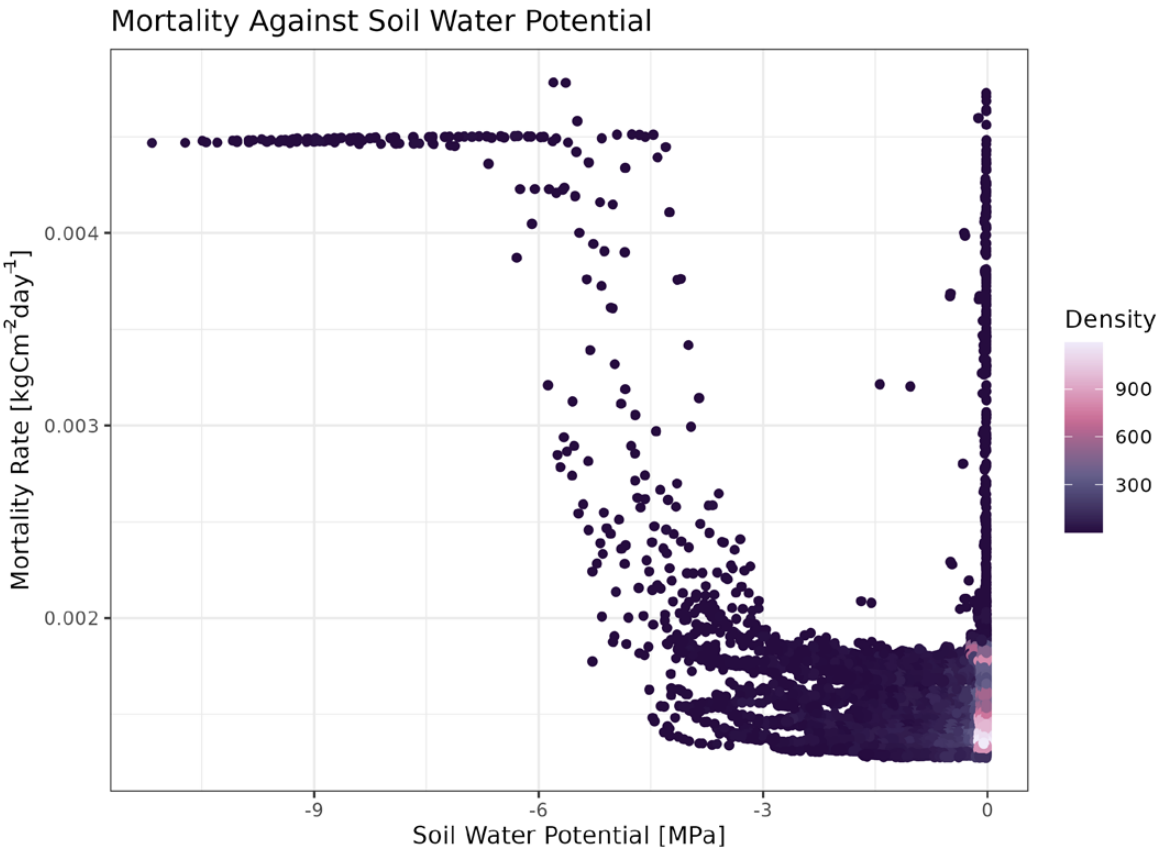


Figure A 13 Mortality rate under different soil water potential values throughout the simulation for randomly selected cells in existing forests (Fig A8) in the most afforested scenario. More negative soil water potential indicates higher water stress. Color indicates kernel density with brighter colours indicative of more points in that part of the plot.

Funding

This paper was funded by the Strategic Initiatives Program, an internal funding program at the International Institute for Applied Systems Analysis. Two SI projects funded this work: RESIST and FairStream.

Author Contributions

EZS led the work with JJ, FH and JdB providing supervision. EZS and JdB implemented the model coupling with inputs from JJ and SM. EZS, SA and JdB parameterised the model and EZS ran simulations. EZS conducted the analysis with inputs from SA and TM. EZS and TM wrote the manuscript and all authors contributed to the writing and approved the final version of the manuscript.

Code and data availability

All models and analysis are open source and freely available.

https://doi.org/10.5194/egusphere-2026-5313
Preprint. Discussion started: 9 November 2026
© Author(s) 2026. CC BY 4.0 License.

The code for the GEB and PantFATE models must be installed separately and ran through the GEB interface. The codebase is available here:

GEB: https://doi.org/10.5281/zenodo.22094305 (Stefaniak and de Bruijn, 2026)

PlantFATE: https://github.com/treehouse-iitb/PlantFATE

The code for the analysis of the results is published separately to accommodate clean software release:

Analysis and model results processing: https://doi.org/10.5281/zenodo.22146184 (Stefaniak et al., 2026a)

Finally, the simulation input data and simulation outputs for the Ghod Subbasin can be found here:

Model settings and model outputs: https://doi.org/10.5281/zenodo.18457345 (Stefaniak et al., 2026b)

Competing interests

The authors declare no competing interests.

Bibliography

Aggarwal, A.: Implementation of Forest Rights Act, changing forest landscape, and "politics of REDD+" in India, Journal of Resources, Energy and Development, 8, 131–148, https://doi.org/10.3233/RED-120089, 2011.

Ai, Z., Hanasaki, N., Heck, V., Hasegawa, T., and Fujimori, S.: Simulating second-generation herbaceous bioenergy crop yield using the global hydrological model H08 (v.bio1), Geoscientific Model Development, 13, 6077–6092, https://doi.org/10.5194/gmd-13-6077-2020, 2020.

Allen, C. D., Macalady, A. K., Chenchouni, H., Bachelet, D., McDowell, N., Vennetier, M., Kitzberger, T., Rigling, A., Breshears, D. D., Hogg, E. H. (Ted), Gonzalez, P., Fensham, R., Zhang, Z., Castro, J., Demidova, N., Lim, J.-H., Allard, G., Running, S. W., Semerci, A., and Cobb, N.: A global overview of drought and heat-induced tree mortality reveals emerging climate change risks for forests, Forest Ecology and Management, 259, 660–684, https://doi.org/10.1016/j.foreco.2009.09.001, 2010.

Anderegg, W. R. L., Trugman, A. T., Badgley, G., Anderson, C. M., Bartuska, A., Ciais, P., Cullenward, D., Field, C. B., Freeman, J., Goetz, S. J., Hicke, J. A., Huntzinger, D., Jackson, R. B., Nickerson, J., Pacala, S., and Randerson, J. T.: Climate-driven risks to the climate mitigation potential of forests, Science, 368, eaaz7005, https://doi.org/10.1126/science.aaz7005, 2020.

Berghuijs, W. R., Collenteur, R. A., Jasechko, S., Jaramillo, F., Luijendijk, E., Moeck, C., Van Der Velde, Y., and Allen, S. T.: Groundwater recharge is sensitive to changing long-term aridity, Nat. Clim. Chang., 14, 357–363, https://doi.org/10.1038/s41558-024-01953-z, 2024.

Brassard, B. W., Chen, H. Y. H., Cavard, X., Laganière, J., Reich, P. B., Bergeron, Y., Paré, D., and Yuan, Z.: Tree species diversity increases fine root productivity through increased soil volume filling, Journal of Ecology, 101, 210–219, https://doi.org/10.1111/1365-2745.12023, 2013.

de Bruijn, J. A., Smilovic, M., Burek, P., Guillaumot, L., Wada, Y., and Aerts, J. C. J. H.: GEB v0.1: a large-scale agent-based socio-hydrological model – simulating 10 million individual farming households in a fully distributed hydrological model, Geoscientific Model Development, 16, 2437–2454, https://doi.org/10.5194/gmd-16-2437-2023, 2023.

de Bruijn, J., Kalthof, M., Bril, V., Tierolf, L., Stefaniak, E., Sadana, T., Busker, T., Oliveira, R., Carral, C., Pontman, R., van Aamelsvoort, L., and Kiesel, J.: GEB: Geographical Environmental and Behavioural model (1.0.0b10), https://docs.geb.sh, 2025.

Buck, A. L.: New Equations for Computing Vapor Pressure and Enhancement Factor, Journal of Applied Meteorology and Climatology, 20, 1527–1532, https://doi.org/10.1175/1520-0450(1981)020<1527:NEFCVP>2.0.CO;2, 1981.

https://doi.org/10.5194/egusphere-2026-5313
Preprint. Discussion started: 9 November 2026
© Author(s) 2026. CC BY 4.0 License.

Burek, P., Satoh, Y., Kahil, T., Tang, T., Greve, P., Smilovic, M., Guillaumot, L., Zhao, F., and Wada, Y.: Development of the Community Water Model (CWatM v1.04) – a high-resolution hydrological model for global and regional assessment of integrated water resources management, Geoscientific Model Development, 13, 3267–3298, https://doi.org/10.5194/gmd-13-3267-2020, 2020.

Bussotti, F. and Pollastrini, M.: Planting Trees as a Nature-Based Solution to Mitigate Climate Change: Opportunities, Limits, and Trade-Offs, Forests, 16, 810, https://doi.org/10.3390/f16050810, 2025.

Calvin, K., Dasgupta, D., Krinner, G., Mukherji, A., Thorne, P. W., Trisos, C., Romero, J., Aldunce, P., Barrett, K., Blanco, G., Cheung, W. W. L., Connors, S., Denton, F., Diongue-Niang, A., Dodman, D., Garschagen, M., Geden, O., Hayward, B., Jones, C., Jotzo, F., Krug, T., Lasco, R., Lee, Y.-Y., Masson-Delmotte, V., Meinshausen, M., Mintenbeck, K., Mokssit, A., Otto, F. E. L., Pathak, M., Pirani, A., Poloczanska, E., Pörtner, H.-O., Revi, A., Roberts, D. C., Roy, J., Ruane, A. C., Skea, J., Shukla, P. R., Slade, R., Slangen, A., Sokona, Y., Sörensson, A. A., Tignor, M., Van Vuuren, D., Wei, Y.-M., Winkler, H., Zhai, P., Zommers, Z., Hourcade, J.-C., Johnson, F. X., Pachauri, S., Simpson, N. P., Singh, C., Thomas, A., Totin, E., Arias, P., Bustamante, M., Elgizouli, I., Flato, G., Howden, M., Méndez-Vallejo, C., Pereira, J. J., Pichs-Madruga, R., Rose, S. K., Saheb, Y., Sánchez Rodríguez, R., Ürge-Vorsatz, D., Xiao, C., Yassaa, N., Alegría, A., Armour, K., Bednar-Friedl, B., Blok, K., Cissé, G., Dentener, F., Eriksen, S., Fischer, E., Garner, G., Guivarch, C., Haasnoot, M., Hansen, G., Hauser, M., Hawkins, E., Hermans, T., Kopp, R., Leprince-Ringuet, N., Lewis, J., Ley, D., Ludden, C., Niamir, L., Nicholls, Z., Some, S., Szopa, S., Trewin, B., Van Der Wijst, K.-I., Winter, G., Witting, M., Birt, A., Ha, M., Romero, J., Kim, J., Haites, E. F., Jung, Y., Stavins, R., Birt, A., Ha, M., Orendain, D. J. A., Ignon, L., Park, S., Park, Y., Reisinger, A., Cammaramo, D., Fischlin, A., Fuglestvedt, J. S., Hansen, G., Ludden, C., Masson-Delmotte, V., Matthews, J. B. R., Mintenbeck, K., Pirani, A., Poloczanska, E., Leprince-Ringuet, N., and Péan, C.: IPCC, 2023: Climate Change 2023: Synthesis Report. Contribution of Working Groups I, II and III to the Sixth Assessment Report of the Intergovernmental Panel on Climate Change [Core Writing Team, H. Lee and J. Romero (eds.)]. IPCC, Geneva, Switzerland., Intergovernmental Panel on Climate Change (IPCC), https://doi.org/10.59327/IPCC/AR6-9789291691647, 2023.

Choat, B., Jansen, S., Brodribb, T. J., Cochard, H., Delzon, S., Bhaskar, R., Bucci, S. J., Feild, T. S., Gleason, S. M., Hacke, U. G., Jacobsen, A. L., Lens, F., Maherali, H., Martínez-Vilalta, J., Mayr, S., Mencuccini, M., Mitchell, P. J., Nardini, A., Pittermann, J., Pratt, R. B., Sperry, J. S., Westoby, M., Wright, I. J., and Zanne, A. E.: Global convergence in the vulnerability of forests to drought, Nature, 491, 752–755, https://doi.org/10.1038/nature11688, 2012.

Debele, S. E., Leo, L. S., Kumar, P., Sahani, J., Ommer, J., Bucchignani, E., Vranić, S., Kalas, M., Amirzada, Z., Pavlova, I., Shah, M. A. R., Gonzalez-Ollauri, A., and Di Sabatino, S.: Nature-based solutions can help reduce the impact of natural hazards: A global analysis of NBS case studies, Science of The Total Environment, 902, 165824, https://doi.org/10.1016/j.scitotenv.2023.165824, 2023.

Delzon, S. and Loustau, D.: Age-related decline in stand water use: sap flow and transpiration in a pine forest chronosequence, Agricultural and Forest Meteorology, 129, 105–119, https://doi.org/10.1016/j.agrformet.2005.01.002, 2005.

Devi, A. S.: Influence of trees and associated variables on soil organic carbon: a review, Journal of Ecology and Environment, 45, 5, https://doi.org/10.1186/s41610-021-00180-3, 2021.

Dittrich, R., Ball, T., Wreford, A., Moran, D., and Spray, C. J.: A cost-benefit analysis of afforestation as a climate change adaptation measure to reduce flood risk, Journal of Flood Risk Management, 12, e12482, https://doi.org/10.1111/jfr3.12482, 2019.

Fajardo, A. and Piper, F. I.: How to cope with drought and not die trying: Drought acclimation across tree species with contrasting niche breadth, Funct Ecol, 1365-2435.13861, https://doi.org/10.1111/1365-2435.13861, 2021.

Franklin, O., Fransson, P., Hofhansl, F., Jansen, S., and Joshi, J.: Optimal balancing of xylem efficiency and safety explains plant vulnerability to drought, Ecology Letters, 26, 1485–1496, https://doi.org/10.1111/ele.14270, 2023.

Frieler, K., Volkholz, J., Lange, S., Schewe, J., Mengel, M., Del Rocío Rivas López, M., Otto, C., Reyer, C. P. O., Karger, D. N., Malle, J. T., Treu, S., Menz, C., Blanchard, J. L., Harrison, C. S., Petrik, C. M., Eddy, T. D., Ortega-Cisneros, K., Novaglio, C., Rousseau, Y., Watson, R. A., Stock, C., Liu, X., Heneghan, R., Tittensor, D., Maury, O., Büchner, M., Vogt, T., Wang, T., Sun, F., Sauer, I. J., Koch, J., Vanderkelen, I., Jägermeyr, J., Müller, C., Rabin, S., Klar, J., Vega Del Valle, I. D., Lasslop, G., Chadburn, S., Burke, E., Gallego-Sala, A., Smith, N., Chang, J., Hantson, S., Burton, C., Gädeke, A., Li, F., Gosling, S. N., Müller Schmied, H., Hattermann, F., Wang, J., Yao, F., Hickler, T., Marcé, R., Pierson, D., Thiery, W., Mercado-Bettín, D., Ladwig, R., Ayala-Zamora, A. I., Forrest, M., and Bechtold, M.: Scenario setup and forcing data for impact model evaluation and impact attribution within the third round of the Inter-Sectoral Impact Model Intercomparison Project (ISIMIP3a), Geosci. Model Dev., 17, 1–51, https://doi.org/10.5194/gmd-17-1-2024, 2024.

https://doi.org/10.5194/egusphere-2026-5313
Preprint. Discussion started: 9 November 2026
© Author(s) 2026. CC BY 4.0 License.

Gupta, H., Janju, S., Mahajan, A., Singh, C., Sharma, S., and Prajapati, A.: Forests and Agroforestry: Nature-Based Solutions for Climate Change Mitigation, in: Forests and Climate Change: Biological Perspectives on Impact, Adaptation, and Mitigation Strategies, edited by: Singh, H., Springer Nature, Singapore, 421–443, https://doi.org/10.1007/978-981-97-3905-9_21, 2024.

Gurtz, J., Baltensweiler, A., and Lang, H.: Spatially distributed hydrotope-based modelling of evapotranspiration and runoff in mountainous basins, Hydrological Processes, 13, 2751–2768, https://doi.org/10.1002/(SICI)1099-1085(19991215)13:17<2751::AID-HYP897>3.0.CO;2-O, 1999.

Haberstroh, S. and Werner, C.: The role of species interactions for forest resilience to drought, Plant Biology, 24, 1098–1107, https://doi.org/10.1111/plb.13415, 2022.

Hesse, B. D., Goisser, M., Hartmann, H., and Grams, T. E. E.: Repeated summer drought delays sugar export from the leaf and impairs phloem transport in mature beech, Tree Physiology, 39, 192–200, https://doi.org/10.1093/treephys/tpy122, 2019.

Hu, Y., Xiang, W., Schäfer, K. V. R., Lei, P., Deng, X., Forrester, D. I., Fang, X., Zeng, Y., Ouyang, S., Chen, L., and Peng, C.: Photosynthetic and hydraulic traits influence forest resistance and resilience to drought stress across different biomes, Science of The Total Environment, 828, 154517, https://doi.org/10.1016/j.scitotenv.2022.154517, 2022.

Ilstedt, U., Bargués Tobella, A., Bazié, H. R., Bayala, J., Verbeeten, E., Nyberg, G., Sanou, J., Benegas, L., Murdiyarso, D., Laudon, H., Sheil, D., and Malmer, A.: Intermediate tree cover can maximize groundwater recharge in the seasonally dry tropics, Sci Rep, 6, 21930, https://doi.org/10.1038/srep21930, 2016.

Jackson, R. B., Jobbágy, E. G., Avissar, R., Roy, S. B., Barrett, D. J., Cook, C. W., Farley, K. A., le Maitre, D. C., McCarl, B. A., and Murray, B. C.: Trading Water for Carbon with Biological Carbon Sequestration, Science, 310, 1944–1947, https://doi.org/10.1126/science.1119282, 2005.

Jakob, W., Rhinelander, J., and Moldovan, D.: pybind11 – Seamless operability between C++11 and Python, https://pybind11.readthedocs.io/en/stable/, 2017.

Jezeera, A. M.: Variation in plant functional traits across contrasting habitats in a seasonally dry tropical forest in the Northern Western Ghats., BS-MS Thesis, http://dr.iiserpune.ac.in:8080/xmlui/handle/123456789/594, 2016.

Jones, J. A., Wei, X., Archer, E., Bishop, K., Blanco, J. A., Ellison, D., Gush, M. B., McNulty, S. G., van Noordwijk, M., and Creed, I. F.: Forest-Water Interactions Under Global Change, in: Forest-Water Interactions, edited by: Levia, D. F., Carlyle-Moses, D. E., Iida, S., Michalzik, B., Nanko, K., and Tischer, A., Springer International Publishing, Cham, 589–624, https://doi.org/10.1007/978-3-030-26086-6_24, 2020.

Joshi, J., Stocker, B. D., Hofhansl, F., Zhou, S., Dieckmann, U., and Prentice, I. C.: Towards a unified theory of plant photosynthesis and hydraulics, Nat. Plants, https://doi.org/10.1038/s41477-022-01244-5, 2022.

Joshi, J., Hofhansl, F., Singh, S., Stocker, B. D., Brännström, Å., Franklin, O., Blanco, C. C., Aleixo, I. F., Lapola, D., Prentice, I. C., and Dieckmann, U.: Competition for light can drive adverse species-composition shifts in the Amazon Forest under elevated CO2, https://doi.org/10.1101/2023.07.03.547575, 3 July 2023a., 2023.

Joshi, J., Zhang, L., Stefaniak, E. Z., Dieckmann, U., and Brännström, Å.: libpspm: A feature-rich numerical package for solving physiologically structured population models, https://doi.org/10.1101/2023.08.04.551683, 6 August 2023b., 2023.

Kalthof, M. W. M. L., De Bruijn, J., De Moel, H., Kreibich, H., and Aerts, J. C. J. H.: Adaptive behavior of farmers under consecutive droughts results in more vulnerable farmers: a large-scale agent-based modeling analysis in the Bhima basin, India, Nat. Hazards Earth Syst. Sci., 25, 1013–1035, https://doi.org/10.5194/nhess-25-1013-2025, 2025.

Kamble, V. K., Brewer, D., and Oliver, M. E.: Is There a Trade-Off between Forest Expansion and Agriculture?, Land Economics, 101, 304, https://doi.org/10.3368/le.101.3.022924-0020R, 2025.

Kanade, R., Lohakare, K., Bhadbhade, N., Joy, K. J., Thomas, Bejoy. K., Martin, J., and Willaarts, B. A.: Situational Analysis of the Upper Bhima sub-basin in the context of the Water-Food-Biodiversity Nexus, , https://doi.org/10.5281/zenodo.8255959, 2023.

Kattge, J., Bönisch, G., Díaz, S., Lavorel, S., Prentice, I. C., Leadley, P., Tautenhahn, S., Werner, G. D. A., Aakala, T., Abedi, M., Acosta, A. T. R., Adamidis, G. C., Adamson, K., Aiba, M., Albert, C. H., Alcántara, J. M., Alcázar C, C., Aleixo, I., Ali, H.,

https://doi.org/10.5194/egusphere-2026-5313
Preprint. Discussion started: 9 November 2026
© Author(s) 2026. CC BY 4.0 License.

Amiaud, B., Ammer, C., Amoroso, M. M., Anand, M., Anderson, C., Anten, N., Antos, J., Apgaua, D. M. G., Ashman, T., Asmara, D. H., Asner, G. P., Aspinwall, M., Atkin, O., Aubin, I., Baastrup-Spohr, L., Bahalkeh, K., Bahn, M., Baker, T., Baker, W. J., Bakker, J. P., Baldocchi, D., Baltzer, J., Banerjee, A., Baranger, A., Barlow, J., Barneche, D. R., Baruch, Z., Bastianelli, D., Battles, J., Bauerle, W., Bauters, M., Bazzato, E., Beckmann, M., Beeckman, H., Beierkuhnlein, C., Bekker, R., Belfry, G., Belluau, M., Beloiu, M., Benavides, R., Benomar, L., Berdugo-Lattke, M. L., Berenguer, E., Bergamin, R., Bergmann, J., Bergmann Carlucci, M., Berner, L., Bernhardt-Römermann, M., Bigler, C., Bjorkman, A. D., Blackman, C., Blanco, C., Blonder, B., Blumenthal, D., Bocanegra-González, K. T., Boeckx, P., Bohlman, S., Böhning-Gaese, K., Boisvert-Marsh, L., Bond, W., Bond-Lamberty, B., Boom, A., Boonman, C. C. F., Bordin, K., Boughton, E. H., Boukili, V., Bowman, D. M. J. S., Bravo, S., Brendel, M. R., Broadley, M. R., Brown, K. A., Bruelheide, H., Brumnich, F., Bruun, H. H., Bruy, D., Buchanan, S. W., Bucher, S. F., Buchmann, N., Buitenwerf, R., Bunker, D. E., Bürger, J., Burrascano, S., Burslem, D. F. R. P., Butterfield, B. J., Byun, C., Marques, M., Scalon, M. C., Caccianiga, M., Cadotte, M., Cailleret, M., Camac, J., Camarero, J. J., Campany, C., Campetella, G., Campos, J. A., Cano-Arboleda, L., Canullo, R., Carbognani, M., Carvalho, F., Casanoves, F., Castagneyrol, B., Catford, J. A., Cavender-Bares, J., Cerabolini, B. E. L., Cervellini, M., Chacón-Madrigal, E., Chapin, K., Chapin, F. S., Chelli, S., Chen, S., Chen, A., Cherubini, P., Chianucci, F., Choat, B., Chung, K., Chytrý, M., Ciccarelli, D., Coll, L., Collins, C. G., Conti, L., Coomes, D., Cornelissen, J. H. C., Cornwell, W. K., Corona, P., Coyea, M., Craine, J., Craven, D., Cromsigt, J. P. G. M., Csecserits, A., Cufar, K., Cuntz, M., Da Silva, A. C., Dahlin, K. M., Dainese, M., Dalke, I., Dalle Fratte, M., Dang-Le, A. T., Danihelka, J., Dannoura, M., Dawson, S., De Beer, A. J., De Frutos, A., De Long, J. R., Dechant, B., Delagrange, S., Delpierre, N., Derroire, G., Dias, A. S., Diaz-Toribio, M. H., Dimitrakopoulos, P. G., Dobrowolski, M., Doktor, D., Dřevojan, P., Dong, N., Dransfield, J., Dressler, S., Duarte, L., Ducouret, E., Dullinger, S., Durka, W., Duursma, R., Dymova, O., E-Vojtkó, A., Eckstein, R. L., Ejtehadi, H., Elser, J., Emilio, T., Engemann, K., Erfanian, M. B., Erfmeier, A., Esquivel-Muelbert, A., Esser, G., Estiarte, M., Domingues, T. F., Fagan, W. F., Fagúndez, J., Falster, D. S., Fan, Y., Fang, J., Farris, E., Fazlioglu, F., Feng, Y., Fernandez-Mendez, F., Ferrara, C., Ferreira, J., Fidelis, A., Finegan, B., Firn, J., Flowers, T. J., Flynn, D. F. B., Fontana, V., Forey, E., Forgiarini, C., François, L., Frangipani, M., Frank, D., Frenette-Dussault, C., Freschet, G. T., Fry, E. L., Fyllas, N. M., Mazzochini, G. G., Gachet, S., Gallagher, R., Ganade, G., Ganga, F., García-Palacios, P., Gargaglione, V., Garnier, E., Garrido, J. L., De Gasper, A. L., Gea-Izquierdo, G., Gibson, D., Gillison, A. N., Giroldo, A., Glasenhardt, M., Gleason, S., Gliesch, M., Goldberg, E., Göldel, B., Gonzalez-Akre, E., Gonzalez-Andujar, J. L., González-Melo, A., González-Robles, A., Graae, B. J., Granda, E., Graves, S., Green, W. A., Gregor, T., Gross, N., Guerin, G. R., Günther, A., Gutiérrez, A. G., Haddock, L., Haines, A., Hall, J., Hambuckers, A., Han, W., Harrison, S. P., Hattingh, W., Hawes, J. E., He, T., He, P., Heberling, J. M., Helm, A., Hempel, S., Hentschel, J., Hérault, B., Hereş, A., Herz, K., Heuertz, M., Hickler, T., Hietz, P., Higuchi, P., Hipp, A. L., Hirons, A., Hock, M., Hogan, J. A., Holl, K., Honnay, O., Hornstein, D., Hou, E., Hough-Snee, N., Hovstad, K. A., Ichie, T., Igić, B., Illa, E., Isaac, M., Ishihara, M., Ivanov, L., Ivanova, L., Iversen, C. M., Izquierdo, J., Jackson, R. B., Jackson, B., Jactel, H., Jagodzinski, A. M., Jandt, U., Jansen, S., Jenkins, T., Jentsch, A., Jespersen, J. R. P., Jiang, G., Johansen, J. L., Johnson, D., Jokela, E. J., Joly, C. A., Jordan, G. J., Joseph, G. S., Junaedi, D., Junker, R. R., Justes, E., Kabzems, R., Kane, J., Kaplan, Z., Kattenborn, T., Kavelenova, L., Kearsley, E., Kempel, A., Kenzo, T., Kerkhoff, A., Khalil, M. I., Kinlock, N. L., Kissling, W. D., Kitajima, K., Kitzberger, T., Kjøller, R., Klein, T., Kleyer, M., Klimešová, J., Klipel, J., Kloeppel, B., Klotz, S., Knops, J. M. H., Kohyama, T., Koike, F., Kollmann, J., Komac, B., Komatsu, K., König, C., Kraft, N. J. B., Kramer, K., Kreft, H., Kühn, I., Kumarathunge, D., Kuppler, J., Kurokawa, H., Kurosawa, Y., Kuyah, S., Laclau, J., Lafleur, B., Lallai, E., Lamb, E., Lamprecht, A., Larkin, D. J., Laughlin, D., Le Bagousse-Pinguet, Y., Le Maire, G., Le Roux, P. C., Le Roux, E., Lee, T., Lens, F., Lewis, S. L., Lhotsky, B., Li, Y., Li, X., Lichstein, J. W., Liebergesell, M., Lim, J. Y., Lin, Y., Linares, J. C., Liu, C., Liu, D., Liu, U., Livingstone, S., Llusià, J., Lohbeck, M., López-García, Á., Lopez-Gonzalez, G., Lososová, Z., Louault, F., Lukács, B. A., Lukeš, P., Luo, Y., Lussu, M., Ma, S., Maciel Rabelo Pereira, C., Mack, M., Maire, V., Mäkelä, A., Mäkinen, H., Malhado, A. C. M., Mallik, A., Manning, P., Manzoni, S., Marchetti, Z., Marchino, L., Marcilio-Silva, V., Marcon, E., Marignani, M., Markesteijn, L., Martin, A., Martínez-Garza, C., Martínez-Vilalta, J., Mašková, T., Mason, K., Mason, N., Massad, T. J., Masse, J., Mayrose, I., McCarthy, J., McCormack, M. L., McCulloh, K., McFadden, I. R., McGill, B. J., McPartland, M. Y., Medeiros, J. S., Medlyn, B., Meerts, P., Mehrabi, Z., Meir, P., Melo, F. P. L., Mencuccini, M., Meredieu, C., Messier, J., Mészáros, I., Metsaranta, J., Michaletz, S. T., Michelaki, C., Migalina, S., Milla, R., Miller, J. E. D., Minden, V., Ming, R., Mokany, K., Moles, A. T., Molnár, A., Molofsky, J., Molz, M., Montgomery, R. A., Monty, A., Moravcová, L., Moreno-Martínez, A., Moretti, M., Mori, A. S., Mori, S., Morris, D., Morrison, J., Mucina, L., Mueller, S., Muir, C. D., Müller, S. C., Munoz, F., Myers-Smith, I. H., Myster, R. W., Nagano, M., Naidu, S., Narayanan, A., Natesan, B., Negoita, L., Nelson, A. S., Neuschulz, E. L., Ni, J., Niedrist, G., Nieto, J., Niinemets, Ü., Nolan, R., Nottebrock, H., Nouvellon, Y., Novakovskiy, A., The Nutrient Network, Nystuen, K. O., O'Grady, A., O'Hara, K., O'Reilly-Nugent, A., Oakley, S., Oberhuber, W., Ohtsuka, T., Oliveira, R., Öllerer, K., Olson, M. E., Onipchenko, V., Onoda, Y., Onstein, R. E., Ordonez, J. C., Osada, N., Ostonen, I., Ottaviani, G., Otto, S., Overbeck, G. E., Ozinga, W. A., Pahl, A. T., Paine, C. E. T., Pakeman, R. J., Papageorgiou, A. C., Parfionova, E., Pärtel, M., Patacca, M., Paula, S., Paule, J., Pauli, H., Pausas, J. G., Peco, B., Penuelas, J., Perea, A., Peri, P. L., Petisco-Souza, A. C., Petraglia, A., Petritan, A. M., Phillips, O. L., Pierce, S., Pillar, V. D., Pisek, J., Pomogaybin, A., Poorter, H., Portsmuth, A., Poschlod, P., Potvin, C., Pounds, D., Powell, A. S., Power, S. A., Prinzing, A., Puglielli, G., Pyšek, P., Raevel, V., Rammig, A., Ransijn, J., Ray, C. A., Reich, P. B., Reichstein, M., Reid, D. E. B., Réjou-Méchain, M., De Dios, V. R., Ribeiro, S., Richardson, S., Riibak, K., Rillig, M. C., Riviera, F., Robert, E. M. R., Roberts, S., Robroek, B., Roddy, A., Rodrigues, A. V., Rogers, A., Rollinson, E., Rolo, V., Römermann, C., Ronzhina, D., Roscher, C., Rosell, J. A., Rosenfield, M. F., Rossi, C., Roy, D. B., Royer-Tardif, S., Rüger, N., Ruiz-Peinado, R., Rumpf, S. B., Rusch, G. M., Ryo, M., Sack, L., Saldaña, A., Salgado-Negret, B., Salguero-Gomez, R., Santa-Regina, I., Santacruz-García, A. C., Santos, J., Sardans, J., Schamp, B., Scherer-Lorenzen, M., Schleuning, M., Schmid, B.,

https://doi.org/10.5194/egusphere-2026-5313
Preprint. Discussion started: 9 November 2026
© Author(s) 2026. CC BY 4.0 License.

Schmidt, M., Schmitt, S., Schneider, J. V., Schowanek, S. D., Schrader, J., Schrodt, F., Schuldt, B., Schurr, F., Selaya Garvizu, G., Semchenko, M., Seymour, C., Sfair, J. C., Sharpe, J. M., Sheppard, C. S., Sheremetiev, S., Shiodera, S., Shipley, B., Shovon, T. A., Siebenkäs, A., Sierra, C., Silva, V., Silva, M., Sitzia, T., Sjöman, H., Slot, M., Smith, N. G., Sodhi, D., Soltis, P., Soltis, D., Somers, B., Sonnier, G., Sørensen, M. V., Sosinski, E. E., Soudzilovskaia, N. A., Souza, A. F., Spasojevic, M., Sperandii, M. G., Stan, A. B., Stegen, J., Steinbauer, K., Stephan, J. G., Sterck, F., Stojanovic, D. B., Strydom, T., Suarez, M. L., Svenning, J., Svitková, I., Svitok, M., Svoboda, M., Swaine, E., Swenson, N., Tabarelli, M., Takagi, K., Tappeiner, U., Tarifa, R., Tauugourdeau, S., Tavsanoglu, C., Te Beest, M., Tedersoo, L., Thiffault, N., Thom, D., Thomas, E., Thompson, K., Thornton, P. E., Thuiller, W., Tichý, L., Tissue, D., Tjoelker, M. G., Tng, D. Y. P., Tobias, J., Török, P., Tarin, T., Torres-Ruiz, J. M., Tóthmérész, B., Treurnicht, M., Trivellone, V., Trolliet, F., Trotsiuk, V., Tsakalos, J. L., Tsiripidis, I., Tysklind, N., Umehara, T., Usoltsev, V., Vadeboncoeur, M., Vaezi, J., Valladares, F., Vamosi, J., Van Bodegom, P. M., Van Breugel, M., Van Cleemput, E., Van De Weg, M., Van Der Merwe, S., Van Der Plas, F., Van Der Sande, M. T., Van Kleunen, M., Van Meerbeek, K., Vanderwel, M., Vanselow, K. A., Vårhammar, A., Varone, L., Vasquez Valderrama, M. Y., Vassilev, K., Vellend, M., Veneklaas, E. J., Verbeeck, H., Verheyen, K., Vibrans, A., Vieira, I., Villacís, J., Violle, C., Vivek, P., Wagner, K., Waldram, M., Waldron, A., Walker, A. P., Waller, M., Walther, G., Wang, H., Wang, F., Wang, W., Watkins, H., Watkins, J., Weber, U., Weedon, J. T., Wei, L., Weigelt, P., Weiher, E., Wells, A. W., Wellstein, C., Wenk, E., Westoby, M., Westwood, A., White, P. J., Whitten, M., Williams, M., Winkler, D. E., Winter, K., Womack, C., Wright, I. J., Wright, S. J., Wright, J., Pinho, B. X., Ximenes, F., Yamada, T., Yamaji, K., Yanai, R., Yankov, N., Yguel, B., Zanini, K. J., Zanne, A. E., Zelený, D., Zhao, Y., Zheng, J., Zheng, J., Ziemińska, K., Zirbel, C. R., Zizka, G., Zo-Bi, I. C., Zotz, G., and Wirth, C.: TRY plant trait database – enhanced coverage and open access, Global Change Biology, 26, 119–188, https://doi.org/10.1111/gcb.14904, 2020.

Keller, A. A. and Fox, J.: Giving credit to reforestation for water quality benefits, PLOS ONE, 14, e0217756, https://doi.org/10.1371/journal.pone.0217756, 2019.

Khorchani, M., Nadal-Romero, E., Lasanta, T., and Tague, C.: Natural revegetation and afforestation in abandoned cropland areas: Hydrological trends and changes in Mediterranean mountains, Hydrological Processes, 35, e14191, https://doi.org/10.1002/hyp.14191, 2021.

Knighton, J., Sanchez-Martinez, P., and Anderegg, L.: A Globally Comprehensive Database of Tree Hydraulic and Structural Traits Imputed from Phylogenetic Relationships, https://doi.org/10.5281/zenodo.15009207, 2025.

Kummu, M., Guillaume, J. H. A., de Moel, H., Eisner, S., Flörke, M., Porkka, M., Siebert, S., Veldkamp, T. I. E., and Ward, P. J.: The world's road to water scarcity: shortage and stress in the 20th century and pathways towards sustainability, Sci Rep, 6, 38495, https://doi.org/10.1038/srep38495, 2016.

Landsberg, J. and Sands, P.: Hydrology and Plant Water Relations, in: Terrestrial Ecology, vol. 4, Elsevier, 185–219, https://doi.org/10.1016/B978-0-12-374460-9.00007-X, 2011.

Lee, J. I. and Wolf, S. A.: Critical assessment of implementation of the Forest Rights Act of India, Land Use Policy, 79, 834–844, https://doi.org/10.1016/j.landusepol.2018.08.024, 2018.

Lischke, H., Zimmermann, N. E., Bolliger, J., Rickebusch, S., and Löffler, T. J.: TreeMig: A forest-landscape model for simulating spatio-temporal patterns from stand to landscape scale, Ecological Modelling, 199, 409–420, https://doi.org/10.1016/j.ecolmodel.2005.11.046, 2006.

Lowore, J., Meaton, J., and Wood, A.: African Forest Honey: an Overlooked NTFP with Potential to Support Livelihoods and Forests, Environmental Management, 62, 15–28, https://doi.org/10.1007/s00267-018-1015-8, 2018.

McDowell, N., Pockman, W. T., Allen, C. D., Breshears, D. D., Cobb, N., Kolb, T., Plaut, J., Sperry, J., West, A., Williams, D. G., and Yepez, E. A.: Mechanisms of plant survival and mortality during drought: why do some plants survive while others succumb to drought?, New Phytologist, 178, 719–739, https://doi.org/10.1111/j.1469-8137.2008.02436.x, 2008.

McDowell, N. G.: Mechanisms Linking Drought, Hydraulics, Carbon Metabolism, and Vegetation Mortality, Plant Physiology, 155, 1051–1059, https://doi.org/10.1104/pp.110.170704, 2011.

McDowell, N. G., Sapes, G., Pivovaroff, A., Adams, H. D., Allen, C. D., Anderegg, W. R. L., Arend, M., Breshears, D. D., Brodribb, T., Choat, B., Cochard, H., De Cáceres, M., De Kauwe, M. G., Grossiord, C., Hammond, W. M., Hartmann, H., Hoch, G., Kahmen, A., Klein, T., Mackay, D. S., Mantova, M., Martínez-Vilalta, J., Medlyn, B. E., Mencuccini, M., Nardini, A., Oliveira, R. S., Sala, A., Tissue, D. T., Torres-Ruiz, J. M., Trowbridge, A. M., Trugman, A. T., Wiley, E., and Xu, C.: Mechanisms of woody-plant mortality under rising drought, CO2 and vapour pressure deficit, Nat Rev Earth Environ, 3, 294–308, https://doi.org/10.1038/s43017-022-00272-1, 2022.

https://doi.org/10.5194/egusphere-2026-5313
Preprint. Discussion started: 9 November 2026
© Author(s) 2026. CC BY 4.0 License.

Meinshausen, M., Nicholls, Z. R. J., Lewis, J., Gidden, M. J., Vogel, E., Freund, M., Beyerle, U., Gessner, C., Nauels, A., Bauer, N., Canadell, J. G., Daniel, J. S., John, A., Krummel, P. B., Luderer, G., Meinshausen, N., Montzka, S. A., Rayner, P. J., Reimann, S., Smith, S. J., van den Berg, M., Velders, G. J. M., Vollmer, M. K., and Wang, R. H. J.: The shared socio-economic pathway (SSP) greenhouse gas concentrations and their extensions to 2500, Geoscientific Model Development, 13, 3571–3605, https://doi.org/10.5194/gmd-13-3571-2020, 2020.

Messager, M. L., Lehner, B., Grill, G., Nedeva, I., and Schmitt, O.: Estimating the volume and age of water stored in global lakes using a geo-statistical approach, Nat Commun, 7, 13603, https://doi.org/10.1038/ncomms13603, 2016.

Moos, C., Bebi, P., Schwarz, M., Stoffel, M., Sudmeier-Rieux, K., and Dorren, L.: Ecosystem-based disaster risk reduction in mountains, Earth-Science Reviews, 177, 497–513, https://doi.org/10.1016/j.earscirev.2017.12.011, 2018.

Poggio, L., De Sousa, L. M., Batjes, N. H., Heuvelink, G. B. M., Kempen, B., Ribeiro, E., and Rossiter, D.: SoilGrids 2.0: producing soil information for the globe with quantified spatial uncertainty, SOIL, 7, 217–240, https://doi.org/10.5194/soil-7-217-2021, 2021.

Pretzsch, H., Rötzer, T., Matyssek, R., Grams, T. E. E., Häberle, K.-H., Pritsch, K., Kerner, R., and Munch, J.-C.: Mixed Norway spruce (Picea abies [L.] Karst) and European beech (Fagus sylvatica [L.]) stands under drought: from reaction pattern to mechanism, Trees, 28, 1305–1321, https://doi.org/10.1007/s00468-014-1035-9, 2014.

Rabbai, A., Wendt, D. E., Curioni, G., Quick, S. E., MacKenzie, A. R., Hannah, D. M., Kettridge, N., Ullah, S., Hart, K. M., and Krause, S.: Soil moisture and temperature dynamics in juvenile and mature forest as a result of tree growth, hydrometeorological forcings, and drought, Hydrological Processes, 37, e14919, https://doi.org/10.1002/hyp.14919, 2023.

Rajguru, J. and Kulkarni, H.: Groundwater in the Ghod River Basin: part of the larger Ghod River Basin management study., Advanced Center for Water Resources Development and Management, Pune, 4, https://doi.org/10.13140/RG.2.2.10343.57760/1, 2018.

Rawls, W. J. and Brakensiek, D. L.: Estimation of Soil Water Retention and Hydraulic Properties, in: Unsaturated Flow in Hydrologic Modeling: Theory and Practice, edited by: Morel-Seytoux, H. J., Springer Netherlands, Dordrecht, 275–300, https://doi.org/10.1007/978-94-009-2352-2_10, 1989.

Rawls, W. J., Pachepsky, Y. A., Ritchie, J. C., Sobecki, T. M., and Bloodworth, H.: Effect of soil organic carbon on soil water retention, Geoderma, 116, 61–76, https://doi.org/10.1016/S0016-7061(03)00094-6, 2003.

Ren, R., Zhang, B., Xu, Q., Gao, D., Xu, W., and Diao, K.: Forest age and precipitation magnitude affected the contribution rate of rainfall to soil water, Plant and Soil, 512, 121–135, https://doi.org/10.1007/s11104-024-06915-0, 2025.

Richards, A. E., Forrester, D. I., Bauhus, J., and Scherer-Lorenzen, M.: The influence of mixed tree plantations on the nutrition of individual species: a review, Tree Physiology, 30, 1192–1208, https://doi.org/10.1093/treephys/tpq035, 2010.

Rüegg, J., Moos, C., Gentile, A., Luisier, G., Elsig, A., Prasicek, G., and Otero, I.: An Approach to Evaluate Mountain Forest Protection and Management as a Means for Flood Mitigation, Front. For. Glob. Change, 5, 785740, https://doi.org/10.3389/ffgc.2022.785740, 2022.

Rugendo, M. K., Gichimu, B. M., Mugwe, J. N., Mucheru-Muna, M., and Mugendi, D. N.: Surface runoff and soil erosion from Nitisols and Ferralsols as influenced by different soil organic carbon levels under simulated rainfall conditions, Heliyon, 9, https://doi.org/10.1016/j.heliyon.2023.e17684, 2023.

Schewe, J., Heinke, J., Gerten, D., Haddeland, I., Arnell, N. W., Clark, D. B., and Kabat, P.: Multimodel assessment of water scarcity under climate change, Proceedings of the National Academy of Sciences, 111, 3245–3250, https://doi.org/10.1073/pnas.1222460110, 2014.

Skubel, R., Arain, M. A., Peichl, M., Brodeur, J. J., Khomik, M., Thorne, R., Trant, J., and Kula, M.: Age effects on the water-use efficiency and water-use dynamics of temperate pine plantation forests, Hydrological Processes, 29, 4100–4113, https://doi.org/10.1002/hyp.10549, 2015.

Sousa-Silva, R., Verheyen, K., Ponette, Q., Bay, E., Sioen, G., Titeux, H., Van de Peer, T., Van Meerbeek, K., and Muys, B.: Tree diversity mitigates defoliation after a drought-induced tipping point, Global Change Biology, 24, 4304–4315, https://doi.org/10.1111/gcb.14326, 2018.

https://doi.org/10.5194/egusphere-2026-5313
Preprint. Discussion started: 9 November 2026
© Author(s) 2026. CC BY 4.0 License.

Speich, M. J. R., Zappa, M., Scherstjanoi, M., and Lischke, H.: FORests and HYdrology under Climate Change in Switzerland v1.0: a spatially distributed model combining hydrology and forest dynamics, Geosci. Model Dev., 13, 537–564, https://doi.org/10.5194/gmd-13-537-2020, 2020.

Stavi, I., Xu, C., and Argaman, E.: Climate-smart forestry in the world's drylands: A review of challenges and opportunities, The Anthropocene Review, 11, 67–90, https://doi.org/10.1177/20530196231182354, 2024.

Stefaniak, E. and de Bruijn, J. A.: GEB a large-scale agent-based socio-hydrological model – simulating 10 million individual farming households in a fully distributed hydrological model (v0.4), https://doi.org/10.5281/zenodo.22094305, 2026.

Stefaniak, E. Z., Joshi, J., Artuso, S., Maxwell, T. L., Smilovic, M., Hofhansl, F., and de Bruijn, J. A.: bhima_processing: analysis code for GEB-PlantFATE v1.0 afforestation scenarios (publication_analysis), https://doi.org/10.5281/zenodo.22146184, 2026a.

Stefaniak, E. Z., Joshi, J., Artuso, S., Maxwell, T. L., Smilovic, M., Hofhansl, F., and de Bruijn, J.: GEB-PlantFATE v1.0 — Afforestation scenario outputs, Ghod subbasin, India, https://doi.org/10.5281/ZENODO.18457345, 2026b.

Stefaniak, E. Z., Tissue, D. T., Falster, D. S., and Medlyn, B. E.: Greater variability in environmental stress favours trees that prioritise storage of carbohydrate reserves over growth: a modelling analysis, https://doi.org/10.5194/egusphere-2026-1474, 10 April 2026c., 2026.

Sunny, R.: Hydraulic traits in seasonally dry tropical forests, PhD Thesis, Dept. of Biology, http://dr.iiserpune.ac.in:8080/jspui/handle/123456789/6128, 2020.

Surinaidu, L., Bacon, C. G. D., and Pavelic, P.: Agricultural groundwater management in the Upper Bhima Basin, India: current status and future scenarios, Hydrology and Earth System Sciences, 17, 507–517, https://doi.org/10.5194/hess-17-507-2013, 2013.

Sutanudjaja, E. H., Van Beek, R., Wanders, N., Wada, Y., Bosmans, J. H. C., Drost, N., Van Der Ent, R. J., De Graaf, I. E. M., Hoch, J. M., De Jong, K., Karssenberg, D., López López, P., Peßenteiner, S., Schmitz, O., Straatsma, M. W., Vannametee, E., Wisser, D., and Bierkens, M. F. P.: PCR-GLOBWB 2: a 5 arcmin global hydrological and water resources model, Geosci. Model Dev., 11, 2429–2453, https://doi.org/10.5194/gmd-11-2429-2018, 2018.

Trabucco, A., Zomer, R. J., Bossio, D. A., van Straaten, O., and Verchot, L. V.: Climate change mitigation through afforestation/reforestation: A global analysis of hydrologic impacts with four case studies, Agriculture, Ecosystems & Environment, 126, 81–97, https://doi.org/10.1016/j.agee.2008.01.015, 2008.

Van Der Knijff, J. M., Younis, J., and De Roo, A. P. J.: LISFLOOD: a GIS-based distributed model for river basin scale water balance and flood simulation, International Journal of Geographical Information Science, 24, 189–212, https://doi.org/10.1080/13658810802549154, 2010.

Verheyen, K., Gillerot, L., Blondeel, H., De Frenne, P., De Pauw, K., Depauw, L., Lorer, E., Sanczuk, P., Schreel, J., Vanneste, T., Wei, L., and Landuyt, D.: Forest canopies as nature-based solutions to mitigate global change effects on people and nature, Journal of Ecology, 112, 2451–2461, https://doi.org/10.1111/1365-2745.14345, 2024.

Vico, G., Thompson, S. E., Manzoni, S., Molini, A., Albertson, J. D., Almeida-Cortez, J. S., Fay, P. A., Feng, X., Guswa, A. J., Liu, H., Wilson, T. G., and Porporato, A.: Climatic, ecophysiological, and phenological controls on plant ecohydrological strategies in seasonally dry ecosystems, Ecohydrology, 8, 660–681, https://doi.org/10.1002/eco.1533, 2015.

Wada, Y., van Beek, L. P., van Kempen, C. M., Reckman, J. W. M., Vasak, S., and Bierkens, M. F.: Global depletion of groundwater resources, Geophysical Research Letters, 37, https://doi.org/10.1029/2010GL044571, 2010.

de Wit, A. J. W., Boogaard, H. L., Supit, I., and van den Berg, M. (Eds.): System description of the WOFOST 7.2, cropping systems model, rev. 1.1., Wageningen Environmental Research, Netherlands, https://edepot.wur.nl/522204, 2020.

Zhang, Z., Lu, C., Chen, J., Li, S., Zheng, X., Zhang, L., and Zhang-Zheng, H.: Perturbation of soil organic carbon induced by land-use change from primary forest, Environ. Res. Lett., 19, 124014, https://doi.org/10.1088/1748-9326/ad8668, 2024.